Journal of Medicinal Chemistry

Subscriber access provided by SELCUK UNIV

Article

Discovery of highly selective brain-penetrant vasopressin 1a antagonists for the potential treatment of autism via a chemogenomic and scaffold hopping approach

Hasane Ratni, Mark Rogers-Evans, Caterina Bissantz, Christophe Grundschober, Jean-Luc Moreau, Franz Schuler, Holger Fischer, Ruben Alvarez-Sanchez, and Patrick Schnider

J. Med. Chem., **Just Accepted Manuscript** • Publication Date (Web): 05 Feb 2015

Downloaded from http://pubs.acs.org on February 6, 2015

Just Accepted

"Just Accepted" manuscripts have been peer-reviewed and accepted for publication. They are posted online prior to technical editing, formatting for publication and author proofing. The American Chemical Society provides "Just Accepted" as a free service to the research community to expedite the dissemination of scientific material as soon as possible after acceptance. "Just Accepted" manuscripts appear in full in PDF format accompanied by an HTML abstract. "Just Accepted" manuscripts have been fully peer reviewed, but should not be considered the official version of record. They are accessible to all readers and citable by the Digital Object Identifier (DOI®). "Just Accepted" is an optional service offered to authors. Therefore, the "Just Accepted" Web site may not include all articles that will be published in the journal. After a manuscript is technically edited and formatted, it will be removed from the "Just Accepted" Web site and published as an ASAP article. Note that technical editing may introduce minor changes to the manuscript text and/or graphics which could affect content, and all legal disclaimers and ethical guidelines that apply to the journal pertain. ACS cannot be held responsible for errors or consequences arising from the use of information contained in these "Just Accepted" manuscripts.

ACS Publications
High quality. High impact.

Journal of Medicinal Chemistry is published by the American Chemical Society. 1155 Sixteenth Street N.W., Washington, DC 20036
Published by American Chemical Society. Copyright © American Chemical Society. However, no copyright claim is made to original U.S. Government works, or works produced by employees of any Commonwealth realm Crown government in the course of their duties.

Discovery of highly selective brain-penetrant vasopressin 1a antagonists for the potential treatment of autism via a chemogenomic and scaffold hopping approach

Hasane Ratni, Mark Rogers-Evans*, Caterina Bissantz*, Christophe Grundschober, Jean-Luc Moreau, Franz Schuler, Holger Fischer, Ruben Alvarez Sanchez and Patrick Schnider*

Pharmaceutical Research and Early Development, Roche Innovation Center Basel, F. Hoffmann-La Roche Ltd, Grenzacherstrasse 124, 4070 Basel, Switzerland

ABSTRACT

From a micromolar high throughput screening hit **7**, the successful complementary application of a chemogenomic approach and of a scaffold hopping exercise rapidly led to a low single digit nanomolar human vasopressin 1a (hV1a) receptor antagonist **38**. Initial optimization of the mouse V1a activities delivered suitable tool compounds which demonstrated a V1a mediated central *in vivo* effect. This novel series was further optimized through parallel synthesis with a focus on balancing lipophilicity to achieve robust aqueous solubility while avoiding P-gp mediated efflux. These efforts led to the discovery of the highly potent and selective brain-

penetrant hV1a antagonist RO5028442 (**8**) suitable for human clinical studies in people with autism.

INTRODUCTION

Oxytocin and vasopressin are evolutionarily highly conserved 9-amino acid cyclic peptides, differing only by 2 amino acids. Both peptides are known to play an important role in the regulation of social behavior in animals and humans.[1] Vasopressin release in the rodent brain is increased during stress, induced by social defeat or forced swim test, and causes a passive coping behavior in the later.[2] Peptidic vasopressin 1 (V1) receptor antagonists injected in the amygdala reduce passive coping behavior,[2] like antidepressant drugs, and reduce anxiety in the elevated plus maze when injected in the septum.[3] In human studies, using BOLD magnetic resonance imaging during a face matching task, intranasal vasopressin administration has been shown to modulate the activity of the cingulate cortex and to reduce the connectivity between subgenual and supragenual cingulate. This work points to a potential neural network linking vasopressin to the modulation of social behavior by changing a subgenual, supragenual cingulate and amygdala negative feedback loop.[4] This indicates that vasopressin is increasing the brain response to socially threatening stimuli in humans, in line with the increased threat perception of normal faces after intranasal vasopressin administration.[5]

Three vasopressin G protein coupled receptors are known. V1a, V1b are expressed in rat brain limbic areas, like hypothalamus, amygdala, septum and hippocampus. V1a receptors are expressed in similar human[6] and monkey brain[7] regions with additional expression in cortical areas in comparison to rats. In the periphery V1a is expressed in kidney, liver, platelets and vascular smooth muscle[8] and V1b in pituitary, heart and lung[9]. V2 is mainly expressed in the

kidney, mediating the antidiuretic effects of vasopressin.[8a] The oxytocin receptor is closely related[10] to the vasopressin receptors and mediates the reported pro-social effects of oxytocin.[1] In addition, oxytocin has well known peripheral effects on uterine contraction during parturition and the milk ejection reflex during lactation.

A brain penetrant V1a antagonist may therefore have antidepressant and anxiolytic properties, as well as pro-social effects by modulating the social brain and may thus have potential for the treatment of psychiatric disorders with social emotional dysfunction, including autism, anxiety disorders and schizophrenia. It is important for such a compound not to block the V2 and oxytocin receptors to avoid peripheral side-effects and not to counteract the pro-social effects of oxytocin.

Despite the therapeutic potential of modulating the vasopressin system in the brain, the number of selective small molecule V1a receptor antagonists reported so far is limited.[11] Compounds which progressed to clinical trials included relcovaptan (SR49059, **1**),[12] a peripherally active molecule from Sanofi-Aventis which has shown initial positive results in the treatment of Raynaud's disease, dysmenorrhoea, and tocolysis,[13] PF-184536 (**2**)[14] from Pfizer targeted on the treatment of dysmenorrhea, and two CNS penetrating compounds from Azevan, SRX-246 (**3**)[15] and SRX-251 (**4**)[16] (Figure 1). In a human fMRI study **3** blocked the effect of intranasal vasopressin on the neural response to angry faces. Secondary analyses revealed furthermore that **3** treatment was associated with significantly attenuated BOLD responses to angry faces in the right temporoparietal junction, precuneus, anterior cingulate, and putamen.[15c] In 2014 a 12-week Phase II clinical trial with **3** for the treatment of Intermittent Explosive Disorder was launched.[17] At a pre-clinical stage, Johnson and Johnson demonstrated *in vivo* efficacy of **5** (JNJ-17308616) in a rat model of anxiety.[18] More recently, MSD disclosed a novel

series of CNS penetrant V1a antagonists exemplified by **6** with a good affinity for the rat receptor.[19] Peripheral *in vivo* functional V1a antagonism was demonstrated by the reversal of V1a mediated arginine vasopressin (AVP) induced blood pressure increases in conscious rats.

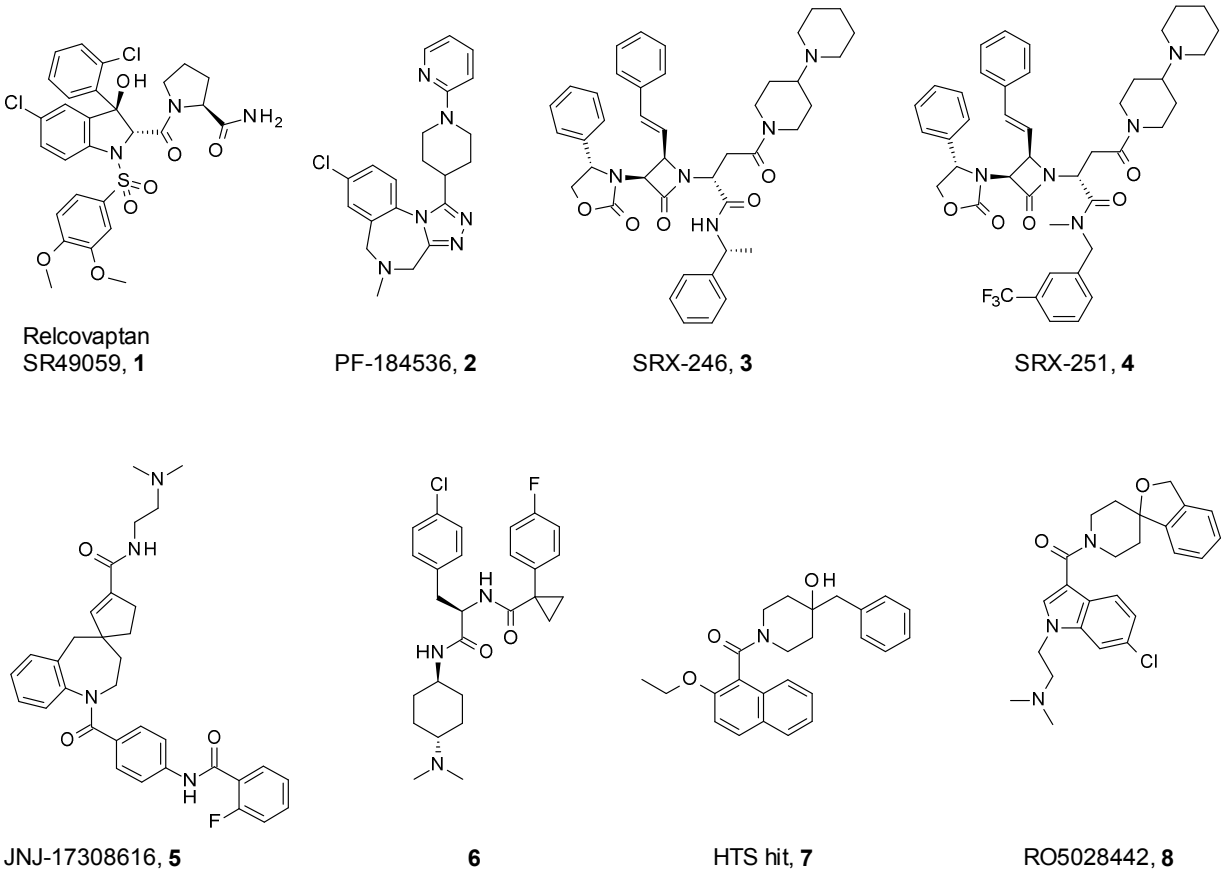

Figure 1. Structure of compounds **1-6**, HTS hit **7** and **8** (RO5028442)

To identify novel starting points for the discovery of an orally bioavailable, CNS penetrant and selective V1a antagonist ligand, we performed a high throughput screening (HTS) campaign of our library using a functional FLIPR assay. We screened around seven hundred thousand compounds at a single concentration of 10μM and obtained a hit rate of 1.48%. Binding affinities of the confirmed hits were determined on both human V1a (hV1a) and human V1b (hV1b) with a Scintillation Proximity Assay (SPA). All hits identified displayed a much

greater affinity for the V1a rather than the V1b receptor. The binding selectivity versus human V2 and oxytocin receptors (hOTR) were also determined. Compound **7** which had binding affinities of 2830 nM and 12000 nM for hV1a and hV1b receptors, respectively, particularly caught our attention due to its high chemical tractability. An efficient combination of chemogenomic and parallel library synthesis methods with a focus on optimization of *in vitro* affinity at the human V1a receptor as well as physicochemical and DMPK properties quickly led to the discovery of **8** suitable for human clinical studies (Figure 1).

RESULTS AND DISCUSSION

Chemistry.

The synthesis of the derivatives described in Table 2 was performed in three steps starting from the commercially available 6-chloro-1H-indole **9** (Scheme 1).[20] Regioselective acetylation using trifluoroacetic anhydride in DMF yielded exclusively the substituted 3-trifluoroacetylindole derivative **10**.[21] This reaction was readily performed on a 50-gram scale with 83% isolated yield. We found that this procedure could be applied to numerous electron rich or poor *N*-unsubstituted indoles, whereas aza-indoles and *N*-substituted indoles could only be acylated when activated with electron donating substituents. Upon treatment with an aqueous solution of sodium hydroxide at reflux, the corresponding substituted indole 3-carboxylic acid **11** was obtained. This versatile key intermediate was ultimately prepared on a hundred-gram scale. Finally, derivatives **12-23** were obtained in high yields by standard amide coupling upon reaction of **11** with a range of amines (called 'head groups' herein after), commercial or readily prepared, such as spiropiperidines, piperidines or piperazines in the presence of HOBt and EDC. Alternatively, the carboxylic acid moiety was converted into an acid chloride prior to reaction with the amines to give **12-23**.

Scheme 1. Synthesis of compounds described in Table 2[a]

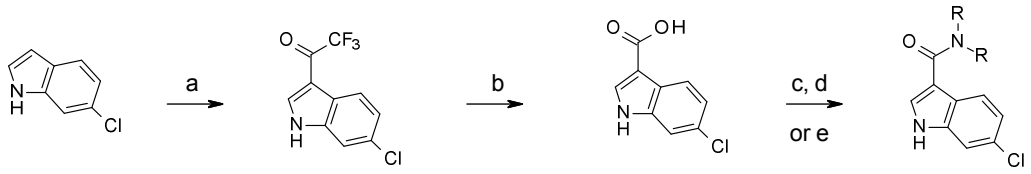

[a]Reagents and conditions: (a) TFAA, DMF, RT, 1h; (b) aq. NaOH, 70 ºC, 16h; (c) oxalyl chloride, DMF, THF; (d) $(R)_2NH$, Et_3N, RT; (e) $(R)_2NH$, HOBt, EDC, CH_2Cl_2, RT.

Subsequent elaboration of *N*-substituted indole was easily performed starting from **12** to provide compounds described in Table 3 (Scheme 2).[20b] Compounds **24** and **25** were obtained by indole *N*-alkylation with the corresponding commercially available 2-chloroacetamides. Alternatively, sequential *N*-alkylation with ethyl-2-bromoacetate followed by hydrolysis of the ester gave **26**, which underwent amide coupling with *N′,N′*-dimethylethane-1,2-diamine to form **27**.

Scheme 2. Synthesis of compounds described in Table 3[a]

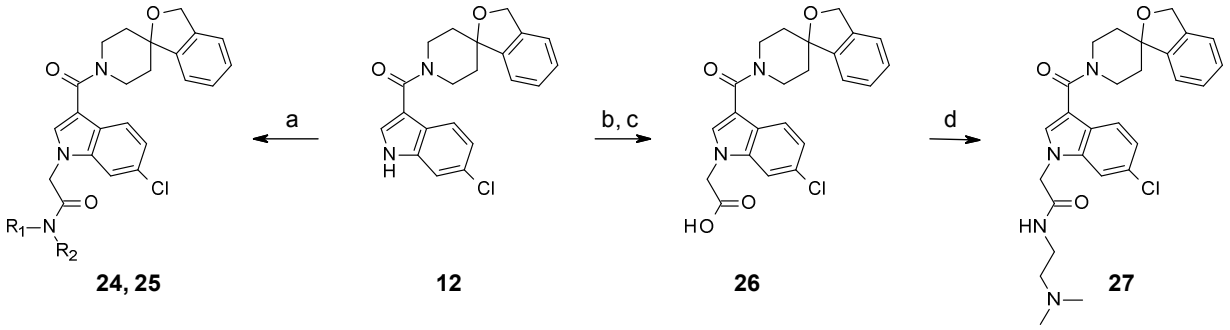

[a]Reagents and conditions: (a) NaH, $R_1R_2NCOCH_2Cl$, DMF (b) NaH, DMF, ethyl-2-bromoacetate, RT; (c) NaOH, H_2O, EtOH, RT; (d) R_1R_2NH, HOBt, EDC, CH_2Cl_2, RT.

The synthesis of the derivatives described in Table 4 started as well from the *N*-unsubstituted indole **12** (Scheme 3).[20b] A straightforward *N*-alkylation with 2-chloro-*N,N*-dimethyl-ethanamine led to **8**, which progressed to clinical studies. This compound was prepared in a total of only four high-yielding steps from the commercially available 6-chloro indole. The other derivatives were prepared via an alkylation with the corresponding mesylate electrophile[22] followed by a reductive amination with aqueous formaldehyde.

Scheme 3. Synthesis of compounds described in Table 4[a]

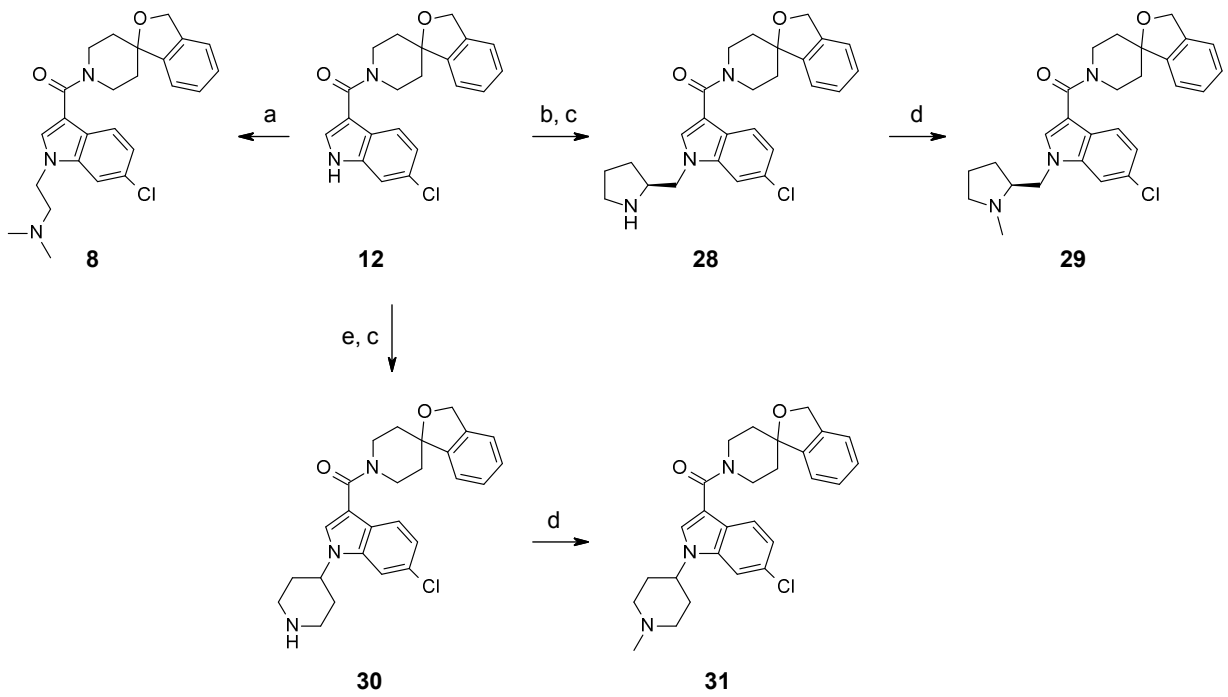

[a]Reagents and conditions: (a) NaH, 2-chloro-*N,N*-dimethyl-ethanamine.HCl, DMF; (b) NaH, tert-butyl (2S)-2-(methylsulfonyloxymethyl)pyrrolidine-1-carboxylate, DMF; (c) TFA, CH_2Cl_2, RT; (d) aq. HCHO, AcOH, $NaBH_3CN$, MeOH; (e) Cs_2CO_3, tert-butyl 4-methylsulfonyloxypiperidine-1-carboxylate, DMF.

Lead optimization.

Chemogenomics allows discovering new ligands for a protein based on a comparison of its binding site with binding sites of other proteins, taking advantage of the idea that proteins with similar binding sites should bind similar ligands. This is a complementary approach to the HTS, which allowed us to virtually screen and identify compounds that were initially not part of an HTS screen. In our search for new antagonists of the V1a receptor we thus clustered all human class A GPCRs based on their binding site similarity with the goal to find another GPCR with a highly similar binding site for which ligands are already known. According to this hypothesis these ligands should have a high probability to also bind to the V1a receptor.

To create the dataset for the chemogenomics approach, all non-olfactory, human class A GPCR receptor sequences were retrieved from the UniProt database.[23] Fragments and sequences were discarded for which not exactly seven transmembrane domains were detected, leading to a total of 298 sequences. We aligned the sequences by a previously published method,[24] and extracted the 35 residues that form the transmembrane pocket (Ligand binding Pocket Vector).[25] We then encoded all residues by descriptors. As descriptors we used the ZZ-scales.[26] Additionally, each residue was described by a set of 5 pharmacophoric descriptors (hydrophobic, aromatic, H-bond donor and/or acceptor, positively ionizable, negatively ionizable). Thus each GPCR was described by a fingerprint of 350 descriptors. Principal Component Analysis was carried out using the SIMCA+10.5 software (Umetrics AB, Umea, Sweden).

Historically, GPCRs are clustered into families based on their natural ligands. GPCRs binding the same natural ligand should have similar binding sites. We thus expect that in our binding-site based clustering, receptors of the same families form clusters (this concept has been validated in-house). This matrix was applied to the search for new V1a antagonists. Figure 2

shows a 3D representation of the matrix around the V1a receptor, and Table 1 shows the distance of the V1a receptor to its closest neighbors.

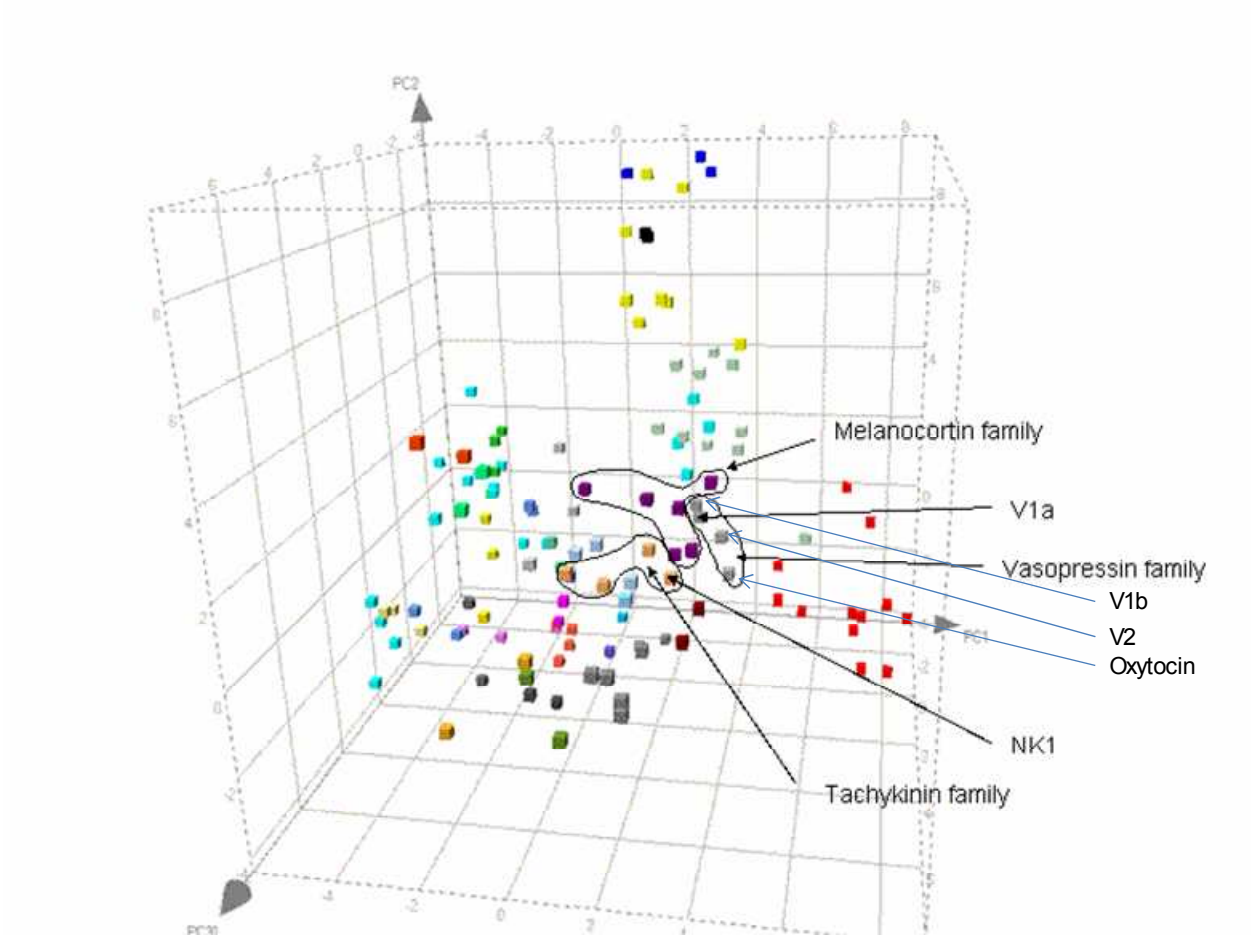

Figure 2. Different colors of the markers represent different GPCR families. The principal components PC1, PC2 and PC3 represent different properties of the binding sites. The largest weight in PC1 have the properties of the residues in the positions 2.58, 6.51, 7.40 and 3.32 according to the Weinstein nomenclature. The largest weight in PC2 have properties in position 5.47, 7.43 and 5.39. Properties of residues 5.47 and 5.39 have a major weight in PC3. However, overall each PC is a mixture of properties of all residues.

Table 1. Nearest neighbor list (top 10 neighbors) of the human V1A receptor.

GPCR name (family)	Distance
GP173 (orphan, SREB)	0.715
MC5R (melanocortin)	0.899
Q8NEN2 (orphan, SREB)	0.901
V1BR (vasopressin-like)	0.924
V2R (vasopressin-like)	0.930
MSHR (melanocortin)	0.937
OXYR (vasopressin-like)	0.950
MC3R (melanocortin)	0.957
NK1R (tachykinin)	1.012
GPR21 (orphan)	1.041

Additionally, two orphan GPCRs are located closely to the vasopressin family (GP173 and Q8NEN2 of the SREB family). From this nearest neighbor list, non-peptidic small molecule ligands are mainly known for the NK1 receptor, a member of the family of mammalian tachykinin receptors, and to a smaller extent for the MSHR receptor. Due to this fact and the in-house availability of different NK1 antagonist series, we decided to select a diverse set of 31 NK1 antagonists for biological testing which were not part of the library we used in the HTS. Nine compounds proved to possess hV1a affinity better than 10000 nM, two of them showed an affinity better than 1000 nM, one of them, **32** had an 81 nM affinity. As this novel hit **32** originated from a NK1 program, we will in course of its optimization for hV1a affinity, monitor closely its side activity on both the NK receptors and the closely associated melanocortin family. Interestingly, the most potent compound differs from our HTS hit **7** only by the substitution of the 4-benzyl-4-hydroxypiperidine with an isomeric spiro analog, leading to a 30-fold increase in *in vitro* hV1a affinity and a marked increase in ligand efficiency from 0.26 to 0.33 (compound **32**, Figure 3). While **7** showed weak affinity for the hV1b receptor, no affinity could be measured for **32**. All compounds tested during the course of optimization of this lead were tested inactive at the hV1b receptor.

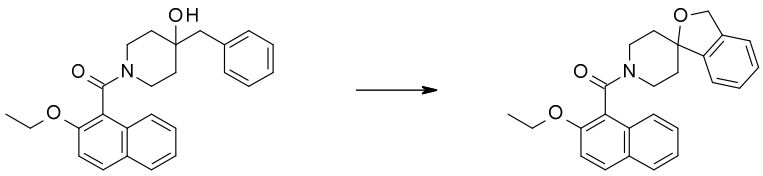

HTS hit, **7**
hV1a Ki: 2830 nM
hV1b Ki: 12000 nM

32
hV1a Ki: 81 nM
hV1b Ki: inactive

Figure 3. Identification of a novel 'head group' via chemogenomics.

In parallel to our chemogenomic approach, we explored the scope of our HTS hit by replacing the 2-ethoxynaphtalene-1-carboxylic acid part in search of further enhanced *in vitro* affinity (Figure 4). Removal of the ethoxy group (**33**) led to a moderate loss of affinity, which can be rationalized by the minor impact of this substituent on the torsional angle between the naphthalene moiety and the amide plane. We next examined the importance of a fused biaryl system by synthesizing a small subset of substituted phenyl derivatives such as **34**. However, a complete loss of affinity was encountered, highlighting the importance of the second aromatic ring. Finally, replacement of the naphthalene moiety with an *N*-benzyl-3-indole fragment led to a tenfold hV1a affinity improvement (e.g. **35**).

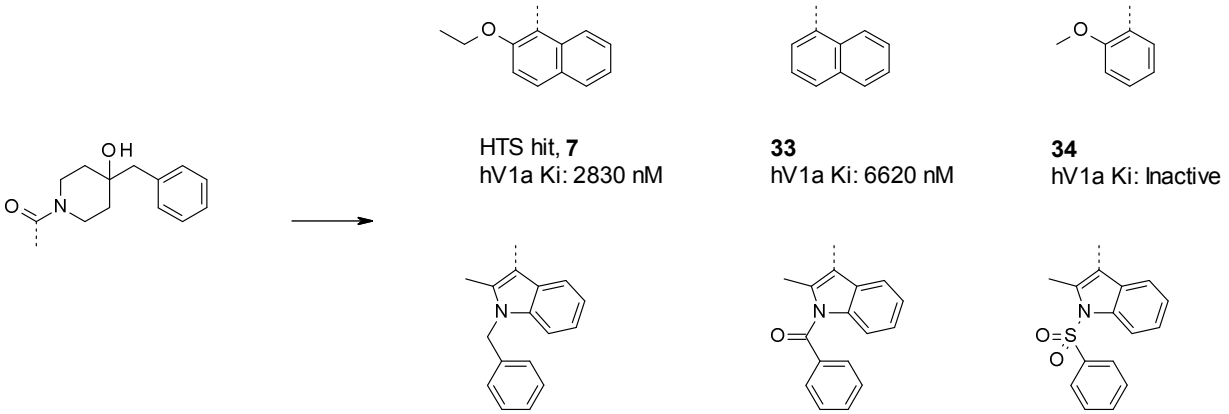

HTS hit, **7**
hV1a Ki: 2830 nM

33
hV1a Ki: 6620 nM

34
hV1a Ki: Inactive

35
hV1a Ki: 295 nM

36
hV1a Ki: 3900 nM

37
hV1a Ki: 4990 nM

Figure 4. Naphthalene scaffold replacement

From the initial hit, the exchange of the head group by a spiropiperidine or the naphthalene replacement by a substituted indole moiety led to a thirty- and ten-fold *in vitro* affinity gain, respectively. Gratifyingly, the combination of these two fragments proved to be synergistic, resulting in the low nanomolar V1a antagonist lead **38**. Starting from an HTS hit with a micromolar affinity, we were thus able to increase the *in vitro* affinity by more than three log units by preparing only two dozen derivatives (Figure 5).

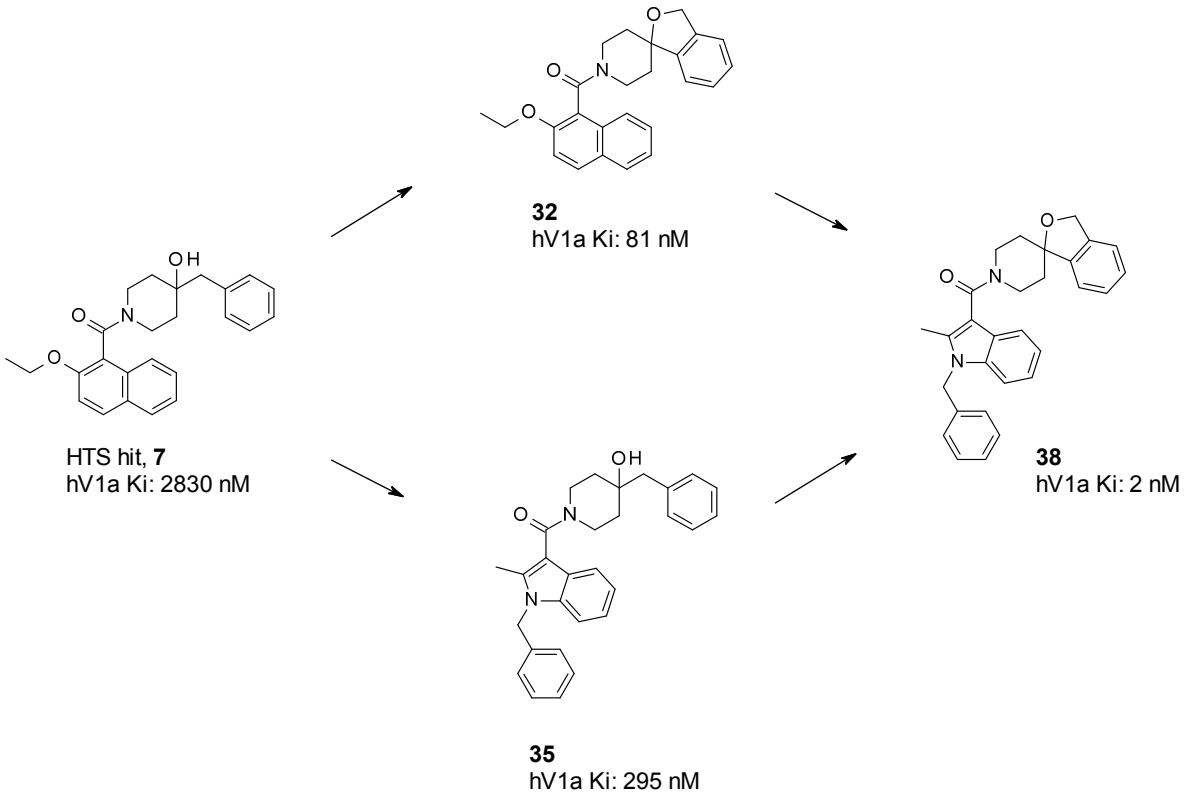

Figure 5. From the micromolar HTS hit **7** to the single digit nanomolar V1a antagonist **38**

Although a high affinity on hV1a was achieved with **38**, this compound suffered from poor aqueous solubility (< 1 μg/mL at pH 6.5) and excessive lipophilicity (kow_cLogP = 5.7, LogD not measurable). Comparison of this compound with the original HTS hit and its close analog **33** (Figure 4) containing only a bare naphthalene moiety suggested that neither the benzyl nor the methyl substituent on the indole were critical (Figure 7). Although the *in vitro* affinity of the unsubstituted indole derivative **39** was reduced, the ligand efficiency (LE) and the lipophilic ligand efficiency (LLE), efficient metrices for lead optimization,[27] as well as the physicochemical properties were markedly improved. Further fine tuning of the indole core restored the *in vitro* affinity upon introduction of a chlorine atom in the 6-position, with compound **12** displaying low nanomolar hV1a affinity and further increased ligand efficiency, high selectivity versus V2 and oxytocin receptors (> 6750 and 1881-fold, respectively) and an improved but not yet satisfactory physico-chemical profile (LogD and solubility) (Figure 6).

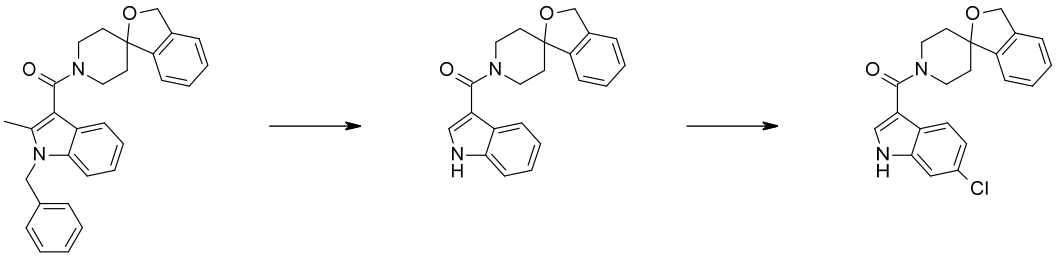

38
hV1a Ki: 2 nM
hV1a Kb: 3.6 nM
mV1a Ki: 210 nM
hV2 Ki: 9308 nM
hOT Ki: Inactive
kow_cLogP: 5.7
LogD: >3
Solubility: <1 mg/L
LE: 0.36
LLE: 3.1

39
hV1a Ki: 32 nM
mV1a Ki: 6620 nM
kow_cLogP: 2.9
LogD: > 3
Solubility: 17 mg/L
LE: 0.41
LLE: 4.6

12
hV1a Ki: 4 nM
hV1a Kb: 2.9 nM
mV1a Ki: 1012 nM
hV2 Ki: > 27000 nM
hOT Ki: 7524 nM
kow_cLogP: 3.7
LogD: 3.7
Solubility: 4 mg/L
LE: 0.44
LLE: 4.8

Figure 6. Optimization of binding and lipophilic ligand efficiency

However, the large species difference between hV1a and mV1a affinity for **12** precluded any *in vivo* behavioral assessment in mice. In search of derivatives with increased mouse V1a affinity, a wide range of analogs with an alternative head group was therefore prepared (Table 2).

Table 2: Head group evaluation

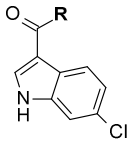

R	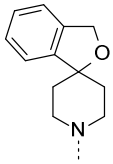	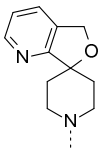	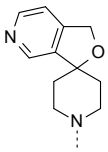	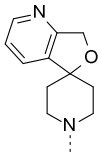	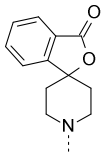	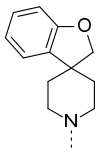
Compd	**12**	**13**	**14**	**15**	**16**	**17**
hV1a Ki (nM)	4	5	9	39	5	16
hV1a Kb (nM)	2.9	1.8	4.2	7.8	5	72
mV1a Ki (nM)	1012	1018	2980	4816	Inactive	Inactive
R	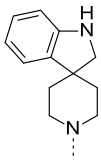	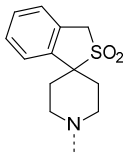	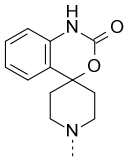	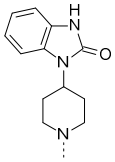	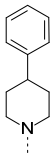	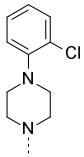
Compd	**18**	**19**	**20**	**21**	**22**	**23**
hV1a Ki (nM)	27	24	32	8	23	118
hV1a Kb (nM)	20	11	38	14	43	193
mV1a Ki (nM)	5890	5886	Inactive	2395	1491	1972

Ki: Binding affinity measured in a radioligand competition binding assay. Kb: Apparent affinity measured in a functional antagonist calcium-flux assay

While high hV1a affinity was achieved with a large diversity of head groups, no improvement of the affinity for neither the human nor the mouse V1a receptor over the spiro[1H-isobenzofuran-3,4'-piperidine] derivative **12** was achieved. We therefore conserved this head group in our next round of optimization.

Interestingly, it was reported that **5** has a high human (5 nM) and much weaker mouse and rat V1a receptor affinity (428 and 216 nM, respectively).[18] However, this species difference for binding affinity was smaller compared to **12**. Furthermore, the modest rodent V1a affinity for **5** was sufficient to demonstrate efficacy in a behavior paradigm of anxiety.[18] A V1a homology model based on the X-ray structure of the bovine rhodopsine receptor was constructed which allowed us to perform ligand-based alignments within the binding pocket between **12** and **5** (Figure 7). The first model was designed by a previously published method.[28] Consequently **5** was manually docked into the binding pocket such that it binds in a low energy conformation. The resulting ligand-receptor complex was consequently minimized. Finally, **12** was docked into the optimized binding pocket in a low energy conformation as well. The resulting ligand alignment clearly indicated the presence of a binding pocket filled by the 2-(*N,N*-dimethylamino)ethyl amide substituent of **5** but not with **12**. The model suggested that the indole nitrogen of **12** is perfectly oriented for the introduction of a substituent to efficiently occupy this pocket. We also tried to rationalized the species affinity difference with this model. However, we could not link the observed differences to one of the specific residue exchanges between the human and mouse receptor sequence.

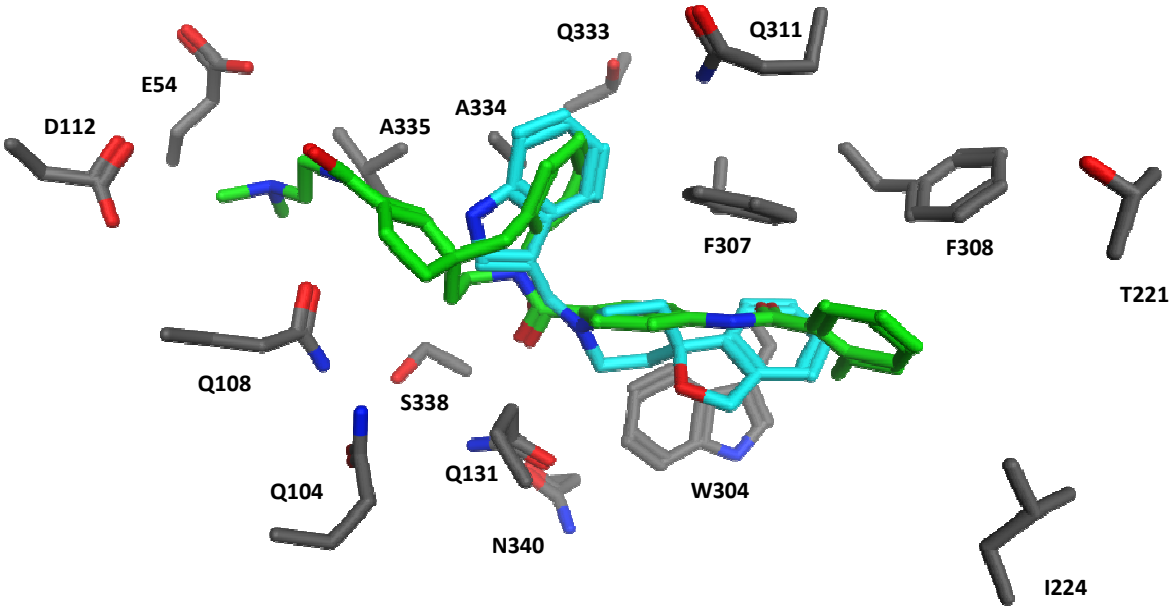

Figure 7. Alignment of **39** and **5** guided by their predicted docking poses to the V1a receptor homology model. Carbon atoms of **39** are depicted in cyan, carbon atoms of **5** in green and those of the receptor in grey. Oxygen atoms are depicted in red, nitrogen atoms in blue.

The introduction of polar acetamide substituents was readily achieved by indole *N*-alkylation. Gratifyingly, this did not only lead to the anticipated increase in solubility but also to a marked improvement of the mouse V1a binding affinity to as low as 14 nM, while the high affinity at the human receptor was retained (Table 3). However, these compounds turned out to be strong substrates of both human and mouse P-glycoprotein (P-gp) . Since all showed high passive permeability, P-gp mediated efflux likely accounts for the poor brain penetration observed in mice.

Table 3: Evaluation of polar amide substituents

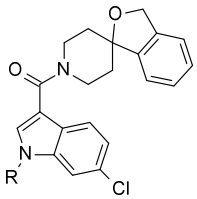

R	H		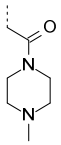	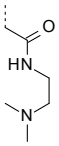
Compd	**12**	**24**	**25**	**27**
hV1a Ki (nM)	4	0.5	1	2
hV1a Kb (nM)	2.9	0.1	0.2	0.7
mV1a Ki (nM)	1012	14	41	177
Binding selectivity vs hV2	> 6750	> 60000	11850	> 15000
Binding selectivity vs hOTR	1881	9160	5690	2214
Solubility (μg/mL)	4	56	193	> 650
hP-gp transport	weak	strong	n.d.	strong
Brain / plasma	n.d.	0.05	0.07	0.1
Vss (l/kg)	n.d.	1.2	1.5	4.9
Cl (mL/min/kg)	n.d.	40	39	14

Ki: Binding affinity measured in a radioligand competition binding assay. Kb: Apparent affinity measured in a functional antagonist calcium-flux assay. Brain/Plasma concentration ratio in mouse @ 10 mg/kg PO. Volume of distribution (Vss) and plasma clearance (Cl) in mouse @ 2 mg/kg i.v.

Central AVP administration stimulates V1a, V1b and oxytocin receptors and induces scratching behavior in mice.[29] In V1a knockout mice AVP does not induce scratching.[30] In order to probe the potential of our new class of V1a receptor antagonists to antagonize brain V1a receptors, **25** was administered to mice i.c.v. prior to the treatment with AVP. Gratifyingly **25** was found to dose-dependently suppress scratching. Based on its superior pharmacokinetic profile due to the lower clearance and higher volume of distribution compared to **24** and **25** we

consequently selected **27** for peripheral i.p. administration. In spite of its poor brain penetration, **27** also showed a dose-dependent suppression of AVP induced scratching (Figure 8).

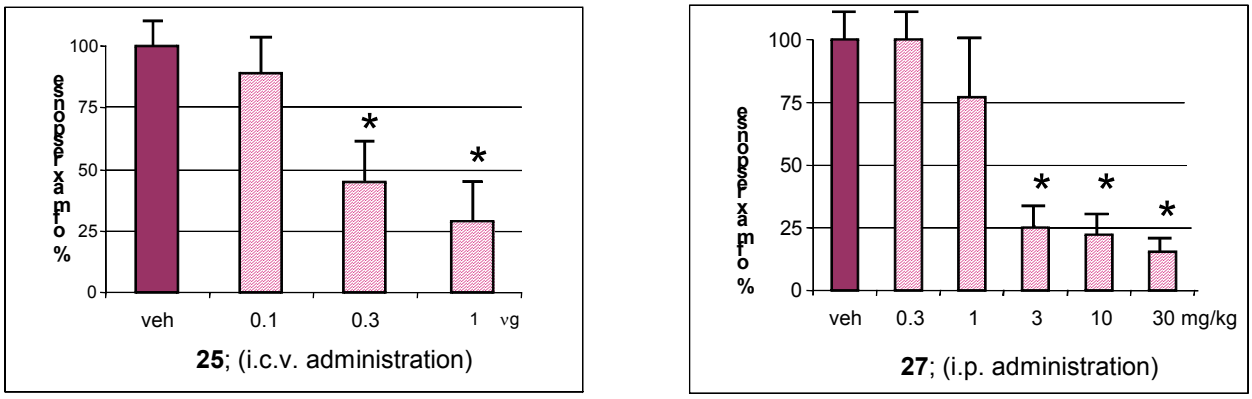

Figure 8. Inhibition AVP-induced scratching by **25** and **27**

Encouraged by these promising pharmacodynamic results, we were seeking derivatives which are devoid of P-gp mediated efflux while retaining a high human V1a affinity, selectivity and solubility (Table 4). H-Bonding capacity has been described to be a key parameter determining P-gp mediated efflux. We thus envisioned to replace the aminoalkyl acetamide *N*-indole substituents containing two strong H-bond acceptors by aminoalkyl residues comprising only one H-bond acceptor. Derivatives with secondary amine substituents were found to be potent hV1a receptor antagonists, although a drop of affinity at the mV1a receptor was often observed. Unfortunately, as exemplified by pyrrolidine derivative **28**, they were also found to be strong substrates of both human and mouse P-gp resulting in poor brain penetration. In contrast, *N*-alkylation to give rise to the corresponding less strongly H-bonding tertiary amines resulted in derivatives which are devoid of P-gp mediated efflux and consequently showed excellent brain penetration. Compounds **29**, **31** and **8** have excellent binding and functional affinity on hV1a, moderate mouse affinity and excellent selectivity versus hV2 and hOT receptors. All compounds

showed high solubility. The *N,N*-dimethylaminoethyl derivative **8** was found to be highly selective against a panel of 89 targets.[31] Finally, **8** was identified as a suitable compound for clinical studies. The entry into human enabling and clinical studies in people with autism with this compound will be reported elsewhere in due course.

Table 4: Evaluation of polar amine substituents

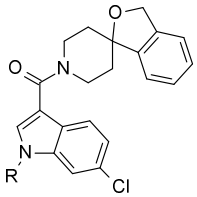

R		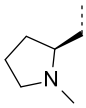	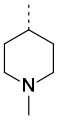	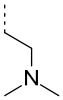
Compd	**28**	**29**	**31**	**8**
hV1a Ki (nM)	1.4	1	4	1
hV1a Kb (nM)	1.4	0.5	3.3	2.6
mV1a Ki (nM)	125	13	11	39
Binding selectivity vs hV2	> 19286	6071	> 6750	> 30000
Binding selectivity vs hOTR	1514	1975	1196	9891
Solubility (mg/L)	108	140	12	205
hP-gp transport	strong	weak	weak	weak
Brain / plasma	0.05	2	1	1.4
Vss (l/kg)	6.8	2.6	7.2	5.8
Cl (mL/min/kg)	32	67	52	91

Ki: Binding affinity measured in a radioligand competition binding assay. Kb: Apparent affinity measured in a functional antagonist calcium-flux assay. Brain/Plasma concentration ratio in mouse @ 10 mg/kg PO. Volume of distribution (Vss) and plasma clearance (Cl) in mouse @ 2 mg/kg i.v.

SUMMARY AND CONCLUSIONS

A brain penetrant V1a antagonist may have antidepressant and anxiolytic properties, as well as pro-social effects by modulating the social brain. It is important for such a compound not to block the V2 and oxytocin receptors to avoid peripheral side-effects and counteracting the pro-social effects of oxytocin. In our search for an orally bioavailable potential drug fulfilling these criteria, we performed a high throughput screening (HTS) campaign of our library.

Among the few weakly active HTS hits, **7** (hV1a Ki =2830 nM) was considered the most promising. An efficient chemogenomic approach allowed us to identify a novel head group, where the substitution of the 4-benzylpiperidin-4-ol with the isomeric spiropiperidine led to a 30-fold increase in *in vitro* affinity as with **32**. Concomitantly, the replacement of the southern part of the hit, the naphthalene moiety by a substituted indole, led to **35** with a 10-fold *in vitro* affinity improvement. The combination of these two fragments proved to be synergistic resulting in the single-digit nanomolar hV1a antagonist **38**. The affinity of the HTS hit was thus improved by more than three log units after preparing only two dozen derivatives.

V1a antagonists have often been reported to suffer from a large discrepancy between human and rodent affinity. This was also the case for our novel class of indole-3-carboxamide V1a antagonists. Efforts to improve mouse V1a affinity while keeping an overall balanced profile met with only partial success. Nevertheless, we were able to demonstrate *in vivo* central target engagement with tool compounds (**25** and **27**). No compounds from this class were further tested in any *in vivo* model of autism.

Encouraged by these promising pharmacodynamic results, we were seeking derivatives which are devoid of P-gp mediated efflux while retaining high affinity on the human V1a

receptor, selectivity and solubility. These efforts ultimately led to the discovery of **8** which was identified as suitable for clinical studies in people with autism.[32] The entry into human enabling and clinical studies in autistic subjects with this compound will be reported elsewhere in due course.

EXPERIMENTAL SECTION

Compound Synthesis and Characterization. Chemistry.

Reactions were carried out under argon atmosphere. Unless otherwise mentioned, all reagents and chemicals were obtained from commercial suppliers and used without further purification. All reactions were followed by TLC (TLC plates F254, Merck) or LCMS (liquid chromatography-mass spectrometry) analysis. The purity of final compounds as measured by HPLC was at least above 95%. Flash column chromatography was carried out either using cartridges packed with silica gel (Isolute Columns, Telos Flash Columns) or on glass columns on silica gel 60 (32-60 mesh, 60Å). LC high resolution spectra were recorded with a Agilent LC-system consisting of Agilent 1290 high pressure system, a CTC PAL auto sampler and a Agilent 6520 QTOF. The separation was achieved on a Zorbax Eclipse Plus C18 1,7 µm 2.1*50mm column at 55°C; A=0.01% formic acid in Water; B= 0.01% formic acid in acetonitrile at flow 1 mL/min. gradient: 0 min 5%B, 0.3 min 5%B, 4.5 min 99 %B 5 min 99%B. The NMR spectra were measured on a Bruker 600 MHz machine in a 5 mm TCI cryoprobe at 298 K. TMS was used for referencing.

[6-Chloro-1-[2-(dimethylamino)ethyl]indol-3-yl]-spiro[1H-isobenzofuran-3,4'-piperidine]-1'-yl-methanone (**8**). To a solution of (6-chloro-1H-indol-3-yl)-spiro[1H-isobenzofuran-3,4'-piperidine]-1'-yl-methanone **12** (50 mg, 0.136 mmol) in DMF (4 mL) cooled at 0 °C, was added sodium hydride dispersion (18 mg, ~55% in oil, 0.41 mmol) and after 0.5h, 2-

chloro-*N,N*-dimethyl-ethanamine hydrochloride (39 mg, 0.34 mmol). After 12h at RT, aqueous NH_4Cl (2 mL) was added and the reaction mixture was concentrated under vacuum. The residue was partitioned between ethyl acetate and water. The organic portion was dried over Na_2SO_4, filtered and concentrated. The crude product was purified by column chromatography, eluting with ethyl acetate to produce **8** (51 mg, 84%) as a white solid. ^{1}H NMR (600 MHz, CHLOROFORM-d) δ 7.68 (d, *J*=8.56 Hz, 1H), 7.55 (s, 1H), 7.36 (d, *J*=1.61 Hz, 1H), 7.27-7.32 (m, 2H), 7.21-7.25 (m, 1H), 7.18 (dd, *J*=1.81, 8.46 Hz, 1H), 7.11-7.14 (m, 1H), 5.11 (s, 2H), 4.41 (br s, 2H), 4.18 (t, *J*=6.90 Hz, 2H), 3.46 (br s, 2H), 2.71 (t, *J*=6.85 Hz, 2H), 2.30 (s, 6H), 1.92 (br s, 2H), 1.79 (br d, *J*=12.89 Hz, 2H); LC-HRMS: m/z = 438.1969 [(M+H)+ calculated for $C_{25}H_{28}ClN_3O_2$ = 438.1943; Diff = 2.6 mD].

1-(6-Chloro-1H-indol-3-yl)-2,2,2-trifluoro-ethanone (**10**). To a solution of 6-chloro-1H-indole **9** (15.0 g, 98.9 mmol) in DMF (150 mL) at 0 °C, was added drop wise trifluoroacetic anhydride (15.8 mL, 114 mmol). After 2 h, another portion of trifluoroacetic anhydride (15.8 mL, 114 mmol) was added, and stirring was continued for an additional 0.5 h. An aqueous saturated sodium carbonate solution (500 mL) was added to the reaction mixture and the product was extracted with three portions (250 mL × 3) of ethyl acetate. The combined organic layers were dried over sodium sulfate and concentrated in vacuo. The residue was triturated in tert.-butyl methyl ether and a filtration produced **10** (20.4 g (82%) as a white solid. The mother liquor was concentrated in vacuo and triturated in tert.-butyl methyl ether followed by filtration gave another portion of **10** (1.2 g, 5%). ^{1}H NMR (600 MHz, CHLOROFORM-d) δ 8.77-9.01 (m, 1H), 8.33 (d, *J*=8.56 Hz, 1H), 8.07 (qd, *J*=1.65, 3.32 Hz, 1H), 7.49 (d, *J*=1.51 Hz, 1H), 7.36 (dd, *J*=1.81, 8.46 Hz, 1H); LC-HRMS: m/z = 245.9960 [(M-H)- calculated for $C_{10}H_5ClF_3NO$ = 245.9939; Diff = 2.1 mD].

6-Chloro-1H-indole-3-carboxylic acid (**11**). A solution of 1-(6-chloro-1H-indol-3-yl)-2,2,2-trifluoro-ethanone (**10**, 21.6 g, 87.2 mmol) in an aqueous solution of potassium hydroxide (4M, 110 mL) was heated at reflux for 2 h. The reaction mixture was cooled to 0 °C and neutralized (final pH of 5) by addition of a concentrated aqueous hydrochloric acid solution (37 mL). The resulting precipitate was collected by filtration, washed with water and dried to afford **11** (16.4 g, 96%) as a white solid. ^{1}H NMR (600 MHz, DMSO-d_6) δ 11.93 (br s, 2H), 8.05 (s, 1H), 8.00 (d, *J*=8.56 Hz, 1H), 7.53 (d, *J*=1.91 Hz, 1H), 7.19 (dd, *J*=1.91, 8.46 Hz, 1H); LC-HRMS: m/z = 194.0024 [(M-H)- calculated for $C_9H_6ClNO_2$ = 194.0014; Diff = 1 mD].

(6-Chloro-1H-indol-3-yl)-spiro[1H-isobenzofuran-3,4'-piperidine]-1'-yl-methanone (**12**). General Procedure A. To a solution of 6-chloro-1H-indole-3-carboxylic acid (**11**, 5 g, 25.6 mmol) in THF (90 mL) was added DMF (39.6 µl, 0.55 mmol). The mixture was cooled to 0 °C and oxalyl dichloride (2.13 mL, 24.3 mmol) was added drop wise. The temperature was raised to RT and stirring was pursued for 3 h, before the mixture was cooled to 5 °C. A solution of spiro[1H-isobenzofuran-3,4'-piperidine][33] (4.99 g, 25.6 mmol) in CH_2Cl_2 (20.0 mL) and triethylamine (7.1 mL, 51.1 mmol) were added. After 0.5 h at RT, the reaction was complete and H_2O (5 mL) was added. The reaction mixture was concentrated under vacuum and the residue taken up in ethyl acetate and washed with water. The organic phase was dried over sodium sulfate, filtered, concentrated before the crude product was purified by flash chromatography eluting with 40% ethyl acetate in heptane to afford **12** (8.2 g, 87%) as a white solid. ^{1}H NMR (600 MHz, CHLOROFORM-d) δ 9.10 (br s, 1H), 7.67 (d, *J*=8.56 Hz, 1H), 7.43 (d, *J*=2.72 Hz, 1H), 7.33 (d, *J*=1.61 Hz, 1H), 7.27-7.31 (m, 2H), 7.21-7.25 (m, 1H), 7.18 (dd, *J*=1.86, 8.51 Hz, 1H), 7.10-7.15 (m, 1H), 5.11 (s, 2H), 4.43 (br d, *J*=11.99 Hz, 2H), 3.48 (br s, 2H), 1.92 (br s,

2H), 1.81 (br s, 2H); LC-HRMS: m/z = 367.1225 [(M+H)+ calculated for $C_{21}H_{19}ClN_2O_2$ = 367.1208; Diff = 1.7 mD].

(6-Chloro-1H-indol-3-yl)-spiro[5H-furo[3,4-b]pyridine-7,4'-piperidine]-1'-yl-methanone (**13**). General procedure A, with **11** (0.03 g, 0.15 mmol) and spiro[5H-furo[3,4-b]pyridine-7,4'-piperidine][20a, 34] (0.032 g, 0.17 mmol), was used to produce **13** (0.039 g, 69%) as a white solid. ^{1}H NMR (600 MHz, CHLOROFORM-d) δ 8.99 (br s, 1H), 8.46-8.55 (m, 1H), 7.67 (d, *J*=8.56 Hz, 1H), 7.58 (dd, *J*=1.31, 7.56 Hz, 1H), 7.43 (d, *J*=2.72 Hz, 1H), 7.35 (d, *J*=1.41 Hz, 1H), 7.21 (dd, *J*=4.94, 7.66 Hz, 1H), 7.18 (dd, *J*=1.81, 8.56 Hz, 1H), 5.11 (s, 2H), 4.40 (br s, 2H), 3.50 (br t, *J*=12.24 Hz, 2H), 2.14 (dt, *J*=4.63, 13.00 Hz, 2H), 1.77 (br d, *J*=12.79 Hz, 2H); LC-HRMS: m/z = 368.118 [(M+H)+ calculated for $C_{20}H_{18}ClN_3O_2$ = 368.1160; Diff = 2 mD].

(6-Chloro-1H-indol-3-yl)-spiro[1H-furo[3,4-c]pyridine-3,4'-piperidine]-1'-yl-methanone (**14**). General procedure A, with **11** (0.03 g, 0.15 mmol) and spiro[1H-furo[3,4-c]pyridine-3,4'-piperidine] (0.032 g, 0.17 mmol), was used to produce **14** (0.038 g, 67%) as a white solid. ^{1}H NMR (600 MHz, CHLOROFORM-d) δ 9.08 (br s, 1H), 8.54 (d, *J*=5.04 Hz, 1H), 8.45 (d, *J*=0.91 Hz, 1H), 7.66 (d, *J*=8.46 Hz, 1H), 7.47 (d, *J*=2.72 Hz, 1H), 7.35 (d, *J*=1.81 Hz, 1H), 7.22 (dd, *J*=0.96, 4.99 Hz, 1H), 7.19 (dd, *J*=1.81, 8.56 Hz, 1H), 5.11 (s, 2H), 4.41 (br s, 2H), 3.49 (br s, 2H), 1.97 (br s, 2H), 1.84 (br d, *J*=12.79 Hz, 2H); LC-HRMS: m/z = 368.1181 [(M+H)+ calculated for $C_{20}H_{18}ClN_3O_2$ = 368.1160; Diff = 2.1 mD].

(6-Chloro-1H-indol-3-yl)-spiro[7H-furo[3,4-b]pyridine-5,4'-piperidine]-1'-yl-methanone (**15**). General procedure A, with **11** (0.03 g, 0.15 mmol) and spiro[7H-furo[3,4-b]pyridine-5,4'-piperidine][20a] (0.032 g, 0.17 mmol), was used to produce **15** (0.054 g, 95%) as a

white solid. ^{1}H NMR (600 MHz, CHLOROFORM-d) δ 8.96 (br s, 1H), 8.51 (dd, *J*=1.41, 4.94 Hz, 1H), 7.67 (d, *J*=8.56 Hz, 1H), 7.46 (d, *J*=2.72 Hz, 1H), 7.44 (dd, *J*=1.41, 7.66 Hz, 1H), 7.36 (d, *J*=1.61 Hz, 1H), 7.17-7.22 (m, 2H), 5.09 (s, 2H), 4.15-4.68 (m, 2H), 3.41-3.64 (m, 2H), 1.71-2.07 (m, 4H); LC-HRMS: m/z = 368.1179 [(M+H)+ calculated for $C_{20}H_{18}ClN_3O_2$ = 368.1160; Diff = 1.9 mD].

1'-(6-Chloro-1H-indole-3-carbonyl)spiro[isobenzofuran-3,4'-piperidine]-1-one (**16**). General procedure A, with **11** (0.150 g, 0.77 mmol) and spiro[isobenzofuran-3,4'-piperidine]-1-one (0.156 g, 0.77 mmol), was used to produce **16** (0.289 g, 99%) as a white solid. ^{1}H NMR (600 MHz, CHLOROFORM-d) δ 8.70 (br s, 1H), 7.92 (d, *J*=7.56 Hz, 1H), 7.66-7.73 (m, 2H), 7.53-7.59 (m, 2H), 7.39-7.43 (m, 2H), 7.23 (dd, *J*=1.76, 8.41 Hz, 1H), 4.52 (br s, 2H), 3.35-3.84 (m, 1H), 3.35-3.84 (m, 1H), 2.17 (br s, 2H), 1.77 (br d, *J*=13.40 Hz, 2H); LC-HRMS: m/z = 381.1001 [(M+H)+ calculated for $C_{21}H_{17}ClN_2O_3$ = 381.1000; Diff = 0.1 mD].

(6-Chloro-1H-indol-3-yl)-spiro[2H-benzofuran-3,4'-piperidine]-1'-yl-methanone (**17**). General Procedure B. To a solution of 6-chloro-1H-indole-3-carboxylic acid (**11**, 0.227 g, 1.16 mmol) in CH_2Cl_2 (15 mL) was added HOBt (0.186 g, 1.50 mmol), EDC (0.263 g, 1.50 mmol) and Et_3N (0.19 mL, 1.50 mmol). The reaction mixture was stirred at 30 °C for 1 h before spiro[2H-benzofuran-3,4'-piperidine] (0.200 g, 1.056 mmol) was added. After 24 h, the mixture was poured into a separating funnel and washed successively with a saturated aqueous ammonium chloride solution, sodium bicarbonate solution and then brine. The organic phase was dried over sodium sulfate, filtered, concentrated before the crude product was purified by flash chromatography eluting with 50% ethyl acetate in heptane to afford **17** (0.191 g, 42%) as a white solid. ^{1}H NMR (600 MHz, CHLOROFORM-d) δ 8.49 (br s, 1H), 7.66 (d, *J*=8.56 Hz, 1H), 7.54 (d, *J*=2.62 Hz, 1H), 7.42 (d, *J*=1.71 Hz, 1H), 7.21 (dd, *J*=1.76, 8.51 Hz, 1H), 7.15-7.18 (m, 1H),

7.14-7.19 (m, 1H), 6.91 (t, *J*=7.10 Hz, 1H), 6.83 (d, *J*=7.66 Hz, 1H), 4.48 (s, 2H), 4.37 (br s, 2H), 3.19 (br t, *J*=12.09 Hz, 2H), 1.89-2.01 (m, 2H), 1.82 (br d, *J*=13.50 Hz, 2H); LC-HRMS: m/z = 365.1086 [(M-H)- calculated for $C_{21}H_{19}ClN_2O_2$ = 365.1062; Diff = 2.4 mD].

(6-Chloro-1H-indol-3-yl)-spiro[indoline-3,4'-piperidine]-1'-yl-methanone (**18**). To a solution of 6-chloro-1H-indole-3-carboxylic acid **11** (0.02 g, 0.10 mmol) and spiro[indoline-3,4'-piperidine] (0.019 g, 0.10 mmol) in DMF (1 mL) at RT was added HATU (0.038 g, 0.10 mmol) and Hunig's base (0.034 mL, 0.2 mmol). After 2h, the reaction was complete and purification by preparative HPLC gave **18** (0.012 g, 35%) as a white solid. ^{1}H NMR (600 MHz, CHLOROFORM-d) δ 8.77 (br s, 1H), 7.66 (d, *J*=8.56 Hz, 1H), 7.47 (d, *J*=2.62 Hz, 1H), 7.37 (d, *J*=1.71 Hz, 1H), 7.19 (dd, *J*=1.86, 8.51 Hz, 1H), 7.10 (s, 1H), 7.05-7.09 (m, 1H), 6.77 (dt, *J*=0.86, 7.43 Hz, 1H), 6.67 (d, *J*=7.66 Hz, 1H), 5.30 (s, 1H), 4.36 (br s, 2H), 3.56 (s, 2H), 3.20 (br t, *J*=11.74 Hz, 2H), 1.89 (br d, *J*=10.28 Hz, 2H), 1.76-1.85 (m, 2H); LC-HRMS: m/z = 366.1378 [(M+H)+ calculated for $C_{21}H_{20}ClN_3O$ = 366.1368; Diff = 1 mD].

(6-Chloro-1H-indol-3-yl)-(2,2-dioxospiro[1H-2-benzothiophene-3,4'-piperidine]-1'-yl)methanone (**19**). General procedure A, with **11** (0.300 g, 1.53 mmol) and spiro[1H-2-benzothiophene-3,4'-piperidine] 2,2-dioxide[35] (0.365 g, 1.53 mmol), was used to produce **19** (0.230 g, 36%) as a white solid. ^{1}H NMR (600 MHz, CHLOROFORM-d) δ 8.49 (br s, 1H), 7.68 (d, *J*=8.66 Hz, 1H), 7.58 (d, *J*=2.72 Hz, 1H), 7.42 (d, *J*=1.81 Hz, 1H), 7.41 (br d, *J*=8.36 Hz, 1H), 7.36 (dt, *J*=1.21, 7.56 Hz, 1H), 7.29 (d, *J*=8.26 Hz, 1H), 7.25 (d, *J*=8.06 Hz, 1H), 7.22 (dd, *J*=1.81, 8.56 Hz, 1H), 4.39 (s, 2H), 4.08-4.59 (m, 2H), 3.54-3.85 (m, 2H), 2.44 (br d, *J*=12.79 Hz, 2H), 2.09 (br d, *J*=10.38 Hz, 2H); LC-HRMS: m/z = 415.0890 [(M+H)+ calculated for $C_{21}H_{19}ClN_2O_3S$ = 415.0878; Diff = 1.2 mD].

1'-(6-Chloro-1H-indole-3-carbonyl)spiro[1H-3,1-benzoxazine-4,4'-piperidine]-2-one (**20**). General procedure B, with **11** (0.024 g, 0.122 mmol) and spiro[1H-3,1-benzoxazine-4,4'-piperidine]-2-one (0.027 g, 0.122 mmol), was used to produce **20** (0.025 g, 51%) as a white solid. ^{1}H NMR (600 MHz, CHLOROFORM-d) δ 8.48 (br s, 1H), 7.66 (d, *J*=8.56 Hz, 1H), 7.57 (d, *J*=2.72 Hz, 1H), 7.43 (d, *J*=1.71 Hz, 1H), 7.27-7.30 (m, 1H), 7.21 (dd, *J*=1.81, 8.56 Hz, 1H), 7.15 (br d, *J*=6.25 Hz, 2H), 7.09-7.12 (m, 1H), 6.78 (d, *J*=7.96 Hz, 1H), 4.09-4.80 (m, 2H), 3.66 (br s, 2H), 2.17 (br d, *J*=13.00 Hz, 2H), 2.05 (br s, 2H); LC-HRMS: m/z = 394.0983 [(M-H)- calculated for $C_{21}H_{18}ClN_3O_3$ = 394.0964; Diff = 1.9 mD].

3-[1-(6-Chloro-1H-indole-3-carbonyl)-4-piperidyl]-1H-benzimidazol-2-one (**21**). General procedure B, with **11** (0.045 g, 0.23 mmol) and 3-(4-piperidyl)-1H-benzimidazol-2-one (0.050 g, 0.23 mmol), was used to produce **21** (0.040 g, 44%) as a white solid. ^{1}H NMR (600 MHz, DMSO-d_6) δ 11.73 (br d, *J*=1.61 Hz, 1H), 10.88 (s, 1H), 7.83 (d, *J*=2.72 Hz, 1H), 7.75 (d, *J*=8.56 Hz, 1H), 7.52 (d, *J*=1.81 Hz, 1H), 7.29 (d, *J*=7.15 Hz, 1H), 7.16 (dd, *J*=1.91, 8.56 Hz, 1H), 6.96-7.07 (m, 3H), 4.29-4.60 (m, 3H), 3.13 (br t, *J*=11.08 Hz, 2H), 2.33 (dq, *J*=4.28, 12.61 Hz, 2H), 1.78 (br d, *J*=10.17 Hz, 2H); LC-HRMS: m/z = 395.1270 [(M+H)+ calculated for $C_{21}H_{19}ClN_4O_2$ = 395.1269; Diff = 0.1 mD].

(6-Chloro-1H-indol-3-yl)-(4-phenyl-1-piperidyl)methanone (**22**). General procedure B, with **11** (20 mg, 0.101 mmol) and 4-phenylpiperidine (16 mg, 0.101 mmol), was used to produce **22** (4.9 mg, 14%) as a white solid. ^{1}H NMR (600 MHz, CHLOROFORM-d) δ 9.23 (br s, 1H), 7.65 (d, *J*=8.56 Hz, 1H), 7.34-7.36 (m, 1H), 7.31-7.34 (m, 1H), 7.30-7.33 (m, 2H), 7.21-7.25 (m, 3H), 7.17 (dd, *J*=1.81, 8.56 Hz, 1H), 4.55 (br s, 2H), 3.07 (br s, 2H), 2.81 (tt, *J*=3.63, 12.14 Hz, 1H), 1.93 (br d, *J*=11.89 Hz, 2H), 1.74 (br d, *J*=11.08 Hz, 2H); LC-HRMS: m/z = 339.1278 [(M+H)+ calculated for $C_{20}H_{19}ClN_2O$ = 339.1259; Diff = 1.9 mD].

(6-Chloro-1H-indol-3-yl)-[4-(2-chlorophenyl)piperazin-1-yl]methanone (**23**). General procedure B, with **11** (36 mg, 0.184 mmol) and 1-(2-chlorophenyl)piperazine (36 mg, 0.184 mmol), was used to produce **23** (24 mg, 35%) as a white solid. ^{1}H NMR (600 MHz, CHLOROFORM-d) δ 8.56 (br s, 1H), 7.67 (d, *J*=8.56 Hz, 1H), 7.53 (d, *J*=2.72 Hz, 1H), 7.41 (d, *J*=1.81 Hz, 1H), 7.38 (dd, *J*=1.51, 7.96 Hz, 1H), 7.22-7.26 (m, 1H), 7.20 (dd, *J*=1.81, 8.56 Hz, 1H), 7.01-7.06 (m, 1H), 6.99-7.03 (m, 1H), 3.91 (br s, 4H), 3.09 (br s, 4H); LC-HRMS: m/z = 374.0831 [(M+H)+ calculated for $C_{19}H_{17}Cl_2N_3O$ = 374.0821; Diff = 1 mD].

2-[6-Chloro-3-(spiro[1H-isobenzofuran-3,4'-piperidine]-1'-carbonyl)indol-1-yl]-*N,N*-dimethyl-acetamide (**24**). To a solution of (6-chloro-1H-indol-3-yl)-spiro[1H-isobenzofuran-3,4'-piperidine]-1'-yl-methanone **12** (60 mg, 0.16 mmol) in DMF (4 mL) cooled at 0 °C, was added sodium hydride dispersion (8 mg, ~55% in oil, 0.17 mmol) and after 0.5h, 2-chloro-*N,N*-dimethyl-acetamide (21 mg, 0.17 mmol). After 2h at RT, aqueous NH_4Cl (2 mL) was added and the reaction mixture was concentrated under vacuum. The residue was partitioned between ethyl acetate and water. The organic portion was dried over Na_2SO_4, filtered and concentrated. The crude product was purified by column chromatography, eluting with ethyl acetate / heptane to produce **24** (13 mg, 18%) as a white solid. ^{1}H NMR (600 MHz, CHLOROFORM-d) δ 7.68 (d, *J*=8.56 Hz, 1H), 7.44 (s, 1H), 7.27-7.31 (m, 2H), 7.24 (d, *J*=1.61 Hz, 1H), 7.21-7.23 (m, 1H), 7.18 (dd, *J*=1.76, 8.51 Hz, 1H), 7.09-7.14 (m, 1H), 5.10 (s, 2H), 4.88 (s, 2H), 4.17-4.61 (m, 2H), 3.49 (s, 2H), 3.13 (s, 3H), 3.02 (s, 3H), 1.92 (br s, 2H), 1.79 (br d, *J*=12.69 Hz, 2H); LC-HRMS: m/z = 452.1752 [(M+H)+ calculated for $C_{25}H_{26}ClN_3O_3$ = 452.1735; Diff = 1.7 mD].

2-[6-Chloro-3-(spiro[1H-isobenzofuran-3,4'-piperidine]-1'-carbonyl)indol-1-yl]-1-(4-methylpiperazin-1-yl)ethanone (**25**). To a solution of (6-chloro-1H-indol-3-yl)-spiro[1H-isobenzofuran-3,4'-piperidine]-1'-yl-methanone **12** (60 mg, 0.16 mmol) in DMF (4 mL) cooled at

0 °C, was added sodium hydride dispersion (8 mg, ~55% in oil, 0.17 mmol) and after 0.5h, 2-chloro-1-(4-methylpiperazin-1-yl)ethanone (30 mg, 0.17 mmol). After 2h at RT, aqueous NH_4Cl (2 mL) was added and the reaction mixture was concentrated under vacuum. The residue was partitioned between ethyl acetate and water. The organic portion was dried over Na_2SO_4, filtered and concentrated. The crude product was purified by column chromatography, eluting with ethyl acetate / heptane to produce **25** (20 mg, 24%) as a white solid. ^{1}H NMR (600 MHz, CHLOROFORM-d) δ 7.68 (d, *J*=8.56 Hz, 1H), 7.43 (s, 1H), 7.27-7.31 (m, 2H), 7.24 (d, *J*=1.71 Hz, 1H), 7.21-7.24 (m, 1H), 7.19 (dd, *J*=1.76, 8.51 Hz, 1H), 7.09-7.14 (m, 1H), 5.10 (s, 2H), 4.88 (s, 2H), 4.43 (br s, 2H), 3.69 (br s, 2H), 3.58 (br s, 2H), 3.46 (br s, 2H), 2.49 (br d, *J*=9.17 Hz, 4H), 2.36 (s, 3H), 1.92 (br s, 2H), 1.79 (br d, *J*=12.39 Hz, 2H); LC-HRMS: m/z = 507.2170 [(M+H)+ calculated for $C_{28}H_{31}ClN_4O_3$ = 507.2157; Diff = 1.3 mD].

2-[6-Chloro-3-(spiro[1H-isobenzofuran-3,4'-piperidine]-1'-carbonyl)indol-1-yl]acetic acid (**26**). Step 1. To a solution of (6-chloro-1H-indol-3-yl)-spiro[1H-isobenzofuran-3,4'-piperidine]-1'-yl-methanone **12** (0.50 g, 1.36 mmol) in DMF (10 mL) cooled at 0 °C, was added sodium hydride dispersion (69 mg, ~50% in oil, 1.43 mmol) and after 0.5h, ethyl 2-bromoacetate (0.16 mL, 1.43 mmol). After 2h at RT, aqueous NH_4Cl (2 mL) was added and the reaction mixture was concentrated under vacuum. The residue was partitioned between ethyl acetate and water. The organic portion was dried over Na_2SO_4, filtered and concentrated. The crude product was purified by column chromatography, eluting with ethyl acetate / heptane to produce ethyl 2-[6-chloro-3-(spiro[1H-isobenzofuran-3,4'-piperidine]-1'-carbonyl)indol-1-yl]acetate (0.56 g, 91%) as a light yellow oil. Step 2. This intermediate was dissolved in EtOH (12 mL) and an aqueous solution of NaOH (1M, 2 mL) was added. The reaction mixture was stirred overnight, before being acidified with HCl (final pH ~3). The resulting solid was

recovered by filtration and washed with water, dried under vacuum to afford **26** (0.44g, 87%) as a white solid and used directly in the next step.

2-[6-Chloro-3-(spiro[1H-isobenzofuran-3,4'-piperidine]-1'-carbonyl)indol-1-yl]-*N*-[2-(dimethylamino)ethyl]acetamide (**27**). To a solution of 2-[6-chloro-3-(spiro[1H-isobenzofuran-3,4'-piperidine]-1'-carbonyl)indol-1-yl]acetic acid **26** (0.150 g, 0.35 mmol) in CH_2Cl_2 (10 mL) was added HOBt (43 mg, 0.35 mmol), EDC (61 mg, 0.35 mmol) and Et_3N (0.044 mL, 0.35 mmol). The reaction mixture was stirred at 30 °C for 1 h before N',N'-dimethylethane-1,2-diamine (31 mg, 0.35 mmol) was added. After 24 h, the mixture was concentrated under vacuum and purification by preparative HPLC gave **27** (64 mg, 37%) as a white solid. ^{1}H NMR (600 MHz, CHLOROFORM-d) δ 7.70 (d, *J*=8.56 Hz, 1H), 7.45 (s, 1H), 7.32 (d, *J*=1.71 Hz, 1H), 7.28-7.31 (m, 2H), 7.21-7.25 (m, 2H), 7.10-7.15 (m, 1H), 6.21 (br s, 1H), 5.11 (s, 2H), 4.77 (s, 2H), 4.39 (br s, 2H), 3.48 (br s, 2H), 3.27 (q, *J*=5.54 Hz, 2H), 2.27 (t, *J*=5.94 Hz, 2H), 2.02 (s, 6H), 1.92 (br d, *J*=10.07 Hz, 2H), 1.81 (br d, *J*=11.38 Hz, 2H); LC-HRMS: m/z = 495.2180 [(M+H)+ calculated for $C_{27}H_{31}ClN_4O_3$ = 495.2157; Diff = 2.3 mD].

[6-Chloro-1-[[(2S)-pyrrolidin-2-yl]methyl]indol-3-yl]-spiro[1H-isobenzofuran-3,4'-piperidine]-1'-yl-methanone (**28**). To a solution of (6-chloro-1H-indol-3-yl)-spiro[1H-isobenzofuran-3,4'-piperidine]-1'-yl-methanone **12** (0.50 g, 1.36 mmol) in DMF (10 mL) cooled at 0 °C, was added sodium hydride dispersion (62 mg, ~55% in oil, 1.43 mmol) and after 0.5h, tert-butyl (2S)-2-(methylsulfonyloxymethyl)pyrrolidine-1-carboxylate (0.38 g, 1.36 mmol). The temperature was raised to 100 °C and after 1h, cooled down to RT before aqueous NH_4Cl (2 mL) was added and the reaction mixture was concentrated under vacuum. The residue was partitioned between ethyl acetate and water. The organic portion was dried over Na_2SO_4, filtered and concentrated. The residue was dissolved in CH_2Cl_2 (3 mL) and TFA (1.5 mL, 14 mmol) was

added and the resulting mixture stirred at RT overnight. The reaction was diluted in ethyl acetate (50 mL) and aqueous $NaHCO_3$ (1M) was added until pH = 8. The organic phase was collected and dried over Na_2SO_4. The crude product was purified by column chromatography, eluting with CH_2Cl_2 / MeOH and aqueous NH_4OH (1%) to produce **28** (0.368 g, 60%) as a white solid. ^{1}H NMR (600 MHz, CHLOROFORM-d) δ 7.69 (d, *J*=8.46 Hz, 1H), 7.58 (s, 1H), 7.41 (d, *J*=1.71 Hz, 1H), 7.27-7.31 (m, 2H), 7.22-7.25 (m, 1H), 7.18 (dd, *J*=1.81, 8.56 Hz, 1H), 7.13 (dd, *J*=3.43, 5.04 Hz, 1H), 5.11 (s, 2H), 4.21-4.63 (m, 2H), 4.15 (dd, *J*=4.94, 14.20 Hz, 1H), 4.05 (dd, *J*=8.01, 14.25 Hz, 1H), 3.55 (ddt, *J*=5.14, 7.45, 7.56 Hz, 1H), 3.47 (br s, 2H), 3.02 (ddd, *J*=5.64, 7.40, 10.23 Hz, 1H), 2.92 (ddd, *J*=6.55, 7.93, 10.20 Hz, 1H), 1.97 (br s, 1H), 1.89-1.97 (m, 2H), 1.82-1.90 (m, 1H), 1.76-1.83 (m, 2H), 1.72-1.80 (m, 1H), 1.46-1.54 (m, 1H); LC-HRMS: m/z = 450.1954 [(M+H)+ calculated for $C_{26}H_{28}ClN_3O_2$ = 450.1943; Diff = 1.1 mD].

[6-Chloro-1-[[(2S)-1-methylpyrrolidin-2-yl]methyl]indol-3-yl]-spiro[1H-isobenzofuran-3,4'-piperidine]-1'-yl-methanone (**29**). To a solution of [6-chloro-1-[[(2S)-pyrrolidin-2-yl]methyl]indol-3-yl]-spiro[1H-isobenzofuran-3,4'-piperidine]-1'-yl-methanone **28** (0.200 g, 0.44 mmol) in MeOH (3.0 mL) was added acetic acid (0.026 mL, 0.462 mmol) and formaldehyde (0.013 mL, 0.462 mmol). Stirring was continued overnight at RT, and $NaBH_3CN$ (0.029 g, 0.462 mmol) was added. After 1h, few drops of water were added and the reaction concentrated under vacuum. The residue was partitioned between ethyl acetate and aqueous $NaHCO_3$. The organic portion was dried over Na_2SO_4, filtered and concentrated. The crude product was purified by column chromatography, eluting with CH_2Cl_2 / MeOH and aqueous NH_4OH (1%) to produce **29** (0.200 g, 96%) as a white solid. ^{1}H NMR (600 MHz, CHLOROFORM-d) δ 7.70 (d, *J*=8.56 Hz, 1H), 7.55 (s, 1H), 7.37 (d, *J*=1.71 Hz, 1H), 7.27-7.32 (m, 2H), 7.21-7.26 (m, 1H), 7.18 (dd, *J*=1.81, 8.56 Hz, 1H), 7.11-7.15 (m, 1H), 5.11 (s, 2H),

4.25-4.64 (m, 2H), 4.18 (br dd, *J*=4.03, 13.40 Hz, 1H), 4.00 (dd, *J*=6.50, 14.25 Hz, 1H), 3.46 (br s, 2H), 3.09 (br s, 1H), 2.62-2.76 (m, 1H), 2.30 (s, 3H), 2.22-2.29 (m, 1H), 1.91 (br d, *J*=18.23 Hz, 2H), 1.81-1.90 (m, 1H), 1.76-1.83 (m, 2H), 1.65-1.74 (m, 2H), 1.50-1.59 (m, 1H); LC-HRMS: m/z = 464.2113 [(M+H)+ calculated for $C_{27}H_{30}ClN_3O_2$ = 464.2099; Diff = 1.4 mD].

[6-Chloro-1-(4-piperidyl)indol-3-yl]-spiro[1H-isobenzofuran-3,4'-piperidine]-1'-yl-methanone (**30**). To a solution of (6-chloro-1H-indol-3-yl)-spiro[1H-isobenzofuran-3,4'-piperidine]-1'-yl-methanone **12** (61 mg, 0.166 mmol) in DMF (1 mL) at RT, was added Cs_2CO_3 (163 mg, 0.50 mmol) and tert-butyl 4-methylsulfonyloxypiperidine-1-carboxylate (140 mg, 0.50 mmol). The reaction mixture was heated at 100 °C overnight and concentrated under vacuum. The residue was partitioned between ethyl acetate and aqueous $NaHCO_3$. The organic portion was dried over Na_2SO_4, filtered and concentrated. The residue was dissolved in CH_2Cl_2 (1 mL) and TFA (0.5 mL, 6.5 mmol) was added and the resulting mixture stirred at RT overnight. The reaction was diluted in ethyl acetate (10 mL) and aqueous $NaHCO_3$ (1M) was added until pH = 8. The organic phase was collected and dried over Na_2SO_4. The crude product was purified by column chromatography, eluting with CH_2Cl_2 / MeOH and aqueous NH_4OH (1%) to produce **30** (51 mg, 68%) as a white solid. ^{1}H NMR (600 MHz, CHLOROFORM-d) δ 7.66 (d, *J*=8.56 Hz, 1H), 7.60 (s, 1H), 7.41 (d, *J*=1.81 Hz, 1H), 7.27-7.32 (m, 2H), 7.21-7.25 (m, 1H), 7.18 (dd, *J*=1.81, 8.56 Hz, 1H), 7.11-7.15 (m, 1H), 5.11 (s, 2H), 4.39 (br s, 2H), 4.26 (tt, *J*=3.98, 11.94 Hz, 1H), 3.47 (br s, 2H), 3.24-3.34 (m, 2H), 2.85 (dt, *J*=2.27, 12.37 Hz, 2H), 2.09-2.17 (m, 2H), 1.97 (br s, 1H), 1.93 (dq, *J*=4.03, 12.26 Hz, 3H), 1.79 (br d, *J*=12.49 Hz, 2H); LC-HRMS: m/z = 450.1963 [(M+H)+ calculated for $C_{26}H_{28}ClN_3O_2$ = 450.1943; Diff = 2 mD].

[6-Chloro-1-(1-methyl-4-piperidyl)indol-3-yl]-spiro[1H-isobenzofuran-3,4'-piperidine]-1'-yl-methanone (**31**). To a stirred solution of [6-chloro-1-(4-piperidyl)indol-3-yl]-

spiro[1H-isobenzofuran-3,4'-piperidine]-1'-yl-methanone (**30**) (21 mg, 0.046 mmol) in MeOH (0.5 mL) was added acetic acid (0.003 mL, 0.051 mmol) and formaldehyde (0.0014 mL, 0.051 mmol). Stirring was continued overnight at RT, and $NaBH_3CN$ (3.2 mg, 0.051 mmol) was added. After 1h, few drops of water were added and the reaction concentrated under vacuum. The residue was partitioned between ethyl acetate and aqueous $NaHCO_3$. The organic portion was dried over Na_2SO_4, filtered and concentrated. The crude product was purified by column chromatography, eluting with CH_2Cl_2 / MeOH and aqueous NH_4OH (1%) to produce **31** (9.5 mg, 44%) as a white solid. ^{1}H NMR (600 MHz, CHLOROFORM-d) δ 7.67 (d, *J*=8.46 Hz, 1H), 7.58 (s, 1H), 7.40 (d, *J*=1.81 Hz, 1H), 7.27-7.31 (m, 2H), 7.21-7.25 (m, 1H), 7.18 (dd, *J*=1.81, 8.56 Hz, 1H), 7.11-7.15 (m, 1H), 5.11 (s, 2H), 4.38 (br s, 2H), 4.08-4.22 (m, 1H), 3.46 (br s, 2H), 3.06 (br d, *J*=12.19 Hz, 2H), 2.38 (s, 3H), 2.21 (td, *J*=7.24, 11.91 Hz, 2H), 2.05-2.16 (m, 4H), 1.92 (br s, 2H), 1.79 (br d, *J*=12.69 Hz, 2H); LC-HRMS: m/z = 464.2113 [(M+H)+ calculated for $C_{27}H_{30}ClN_3O_2$ = 464.2099; Diff = 1.4 mD].

(4-Benzyl-4-hydroxy-1-piperidyl)-(1-naphthyl)methanone (**33**). To a solution of naphthalene-1-carboxylic acid (50 mg, 0.29 mmol) in CH_3CN (6.0 mL) at RT was added Et_3N (0.080 mL, 0.29 mmol), DMAP (6.5 mg, 0.058 mmol) and 4-nitrobenzenesulfonyl chloride (64 mg, 0.29 mmol) at RT. After 0.5h, 4-benzylpiperidin-4-ol (61 mg, 0.319 mmol) was added and stirring continued two more hours. Aqueous $NaHCO_3$ (1M, 2 mL) was added and the reaction partitioned between CH_2Cl_2 and aqueous $NaHCO_3$. The organic portion was dried over Na_2SO_4, filtered and concentrated. The crude product was purified by column chromatography, eluting with heptane / ethyl acetate to produce **33** (26 mg, 26%) as a white solid. ^{1}H NMR (600 MHz, CHLOROFORM-d) δ 7.85-7.92 (m, 2H), 7.83 (d, *J*=7.45 Hz, 1H), 7.76-7.80 (m, 1H), 7.45-7.56 (m, 3H), 7.42-7.45 (m, 1H), 7.37 (dd, *J*=0.86, 7.00 Hz, 1H), 7.30-7.35 (m, 2H), 7.27-7.29 (m,

1H), 7.19 (d, *J*=7.05 Hz, 1H), 7.16 (d, *J*=6.85 Hz, 1H), 4.57-4.85 (m, 1H), 3.23-3.39 (m, 2H), 2.72-2.90 (m, 2H), 1.78-1.95 (m, 1H), 1.71 (dt, *J*=2.62, 14.15 Hz, 1H), 1.50-1.57 (m, 1H), 1.44 (dt, *J*=4.89, 12.87 Hz, 1H), 1.32-1.40 (m, 1H); LC-HRMS: m/z = 346.1824 [(M+H)+ calculated for $C_{23}H_{23}NO_2$ = 346.1802; Diff = 2.2 mD].

(4-Benzyl-4-hydroxy-1-piperidyl)-(2-methoxyphenyl)methanone (**34**). To a stirred solution of 2-methoxybenzoyl chloride (30 mg, 0.175 mmol) in CH_2Cl_2 (3.0 mL) was added 4-benzylpiperidin-4-ol (33 mg, 0.175 mmol) and pyridine (0.042 mL, 0.525 mmol). The reaction mixture was stirred at RT overnight, and partitioned between CH_2Cl_2 and aqueous $NaHCO_3$. The organic portion was dried over Na_2SO_4, filtered and concentrated. The crude product was purified by column chromatography, eluting with ethyl acetate to produce **34** (12 mg, 21%) as a white solid. ^{1}H NMR (600 MHz, CHLOROFORM-d) δ 7.30-7.37 (m, 3H), 7.27-7.30 (m, 1H), 7.24 (dd, *J*=1.51, 7.35 Hz, 1H), 7.14-7.21 (m, 3H), 6.98 (q, *J*=6.95 Hz, 1H), 6.90 (dd, *J*=3.42, 8.26 Hz, 1H), 4.55 (dt, *J*=4.08, 8.54 Hz, 1H), 3.80 (d, *J*=12.49 Hz, 3H), 3.32-3.41 (m, 1H), 3.23-3.30 (m, 1H), 3.08-3.22 (m, 1H), 2.78 (d, *J*=11.28 Hz, 2H), 1.61-1.86 (m, 2H), 1.39-1.54 (m, 2H); LC-HRMS: m/z = 326.1778 [(M+H)+ calculated for $C_{20}H_{23}NO_3$ = 326.1751; Diff = 2.7 mD].

(4-Benzyl-4-hydroxy-1-piperidyl)-(1-benzyl-2-methyl-indol-3-yl)methanone (**35**). In analogy to the procedure used for the preparation of **33**, from 1-benzyl-2-methyl-indole-3-carboxylic acid (50 mg, 0.188 mmol) and 4-benzylpiperidin-4-ol (36 mg, 0.188 mmol) in CH_3CN (4.0 mL) in presence of Et_3N (0.050 mL, 0.377 mmol), DMAP (4.1 mg, 0.038 mmol) and 4-nitrobenzenesulfonyl chloride (41 mg, 0.188 mmol) was produce **35** (31 mg, 37%) as a white solid. The NMR indicated the presence of two rotamers. ^{1}H NMR (600 MHz, CHLOROFORM-d) δ 7.59 (br d, *J*=5.94 Hz) and 7.48 (br s) together 1H, 7.27-7.37 (m, 5H),

7.10-7.25 (m, 6H), 7.01 (br dd, *J*=7.25, 14.71 Hz, 2H), 5.32 (br s, 2H), 3.35-3.54 (m, 2H), 3.30 (br s, 2H), 2.68-2.88 (m, 2H), 2.49 (s) and 2.41 (s) together 3H, 1.76 (br s, 2H), 1.28 (br s, 2H); LC-HRMS: m/z = 439.2398 [(M+H)+ calculated for $C_{29}H_{30}N_2O_2$ = 439.2380; Diff = 1.8 mD].

[3-(4-Benzyl-4-hydroxy-piperidine-1-carbonyl)-2-methyl-indol-1-yl]-phenyl-methanone (**36**). Step 1. General procedure B, with 2-methyl-1H-indole-3-carboxylic acid (1.00 g, 5.71 mmol) and 4-benzylpiperidin-4-ol (1.091 g, 5.71 mmol), was used to produce (4-benzyl-4-hydroxy-1-piperidyl)-(2-methyl-1H-indol-3-yl)methanone (0.80 g, 40%) as a white solid. Step 2. To a solution of (4-benzyl-4-hydroxy-1-piperidyl)-(2-methyl-1H-indol-3-yl)methanone (50 mg, 0.143 mmol) in DMF (5.0 mL) at RT was added a sodium hydride dispersion (5.7 mg, ~60% in oil, 0.143 mmol) and after 0.5h, benzoyl chloride (0.015 mL, 0.171 mmol). After one hour at RT, aqueous NH_4Cl (2 mL) was added and the reaction mixture was concentrated under vacuum. The residue was partitioned between ethyl acetate and water. The organic portion was dried over Na_2SO_4, filtered and concentrated. Purification by preparative HPLC produced **36** (35 mg, 54%) as a white solid. LC-HRMS: m/z = 453.2193 [(M+H)+ calculated for $C_{29}H_{28}N_2O_3$ = 453.2173; Diff = 2 mD].

[1-(Benzenesulfonyl)-2-methyl-indol-3-yl]-(4-benzyl-4-hydroxy-1-piperidyl)methanone (**37**). In analogy to the procedure used for the preparation of **36** (step 2), from (4-benzyl-4-hydroxy-1-piperidyl)-(2-methyl-1H-indol-3-yl)methanone (50 mg, 0.143 mmol) and benzenesulfonyl chloride (0.171 mmol) was prepared **37** (31 mg, 44%) as a white solid. ^{1}H NMR (600 MHz, CHLOROFORM-d) δ 8.20 (dd, *J*=8.46, 12.79 Hz, 1H), 7.83 (dt, *J*=1.21, 7.96 Hz, 2H), 7.53-7.60 (m, 1H), 7.42-7.50 (m, 2H), 7.39 (d, *J*=7.86 Hz, 1H), 7.30-7.36 (m, 3H), 7.27-7.30 (m, 2H), 7.22-7.25 (m, 1H), 7.14-7.21 (m, 2H), 4.54 (br t, *J*=12.09 Hz, 1H), 3.28-3.41 (m, 2H), 3.10-3.27 (m, 1H), 2.77 (s, 2H), 2.50-2.67 (m, 3H), 1.61-1.82 (m, 2H), 1.37-

1.51 (m, 2H); LC-HRMS: m/z = 489.1867 [(M+H)+ calculated for $C_{28}H_{28}N_2O_4S$ = 489.1843; Diff = 2.4 mD].

(1-Benzyl-2-methyl-indol-3-yl)-spiro[1H-isobenzofuran-3,4'-piperidine]-1'-yl-methanone (**38**). In analogy to the procedure used for the preparation of **33**, from 1-benzyl-2-methyl-indole-3-carboxylic acid (50 mg, 0.188 mmol) and spiro[1H-isobenzofuran-3,4'-piperidine] (30 mg, 0.158 mmol) in CH_2Cl_2 (4.0 mL) in presence of Et_3N (0.043 mL, 0.317 mmol), DMAP (3.5 mg, 0.032 mmol) and 4-nitrobenzenesulfonyl chloride (35 mg, 0.158 mmol) was produce **38** (45 mg, 65%) as a white solid. The NMR indicated the presence of two rotamers. ^{1}H NMR (600 MHz, CHLOROFORM-d) δ 7.71 (br d, *J*=7.05 Hz) and 7.52 (br d, *J*=6.85 Hz) together 1H, 7.27-7.33 (m) and 7.21-7.26 (m) together 6H, 7.16 (br s, 3H), 7.09 (br d, *J*=5.14 Hz, 1H), 6.98-7.06 (m, 2H), 5.34 (br s, 2H), 5.10 (br s, 2H), 4.40-4.93 (m, 1H), 3.74-4.27 (m, 1H), 3.25-3.70 (m, 2H), 2.57 (s) and 2.44 (br s) together 3H, 1.63-2.16 (m, 4H); LC-HRMS: m/z = 437.2239 [(M+H)+ calculated for $C_{29}H_{28}N_2O_2$ = 437.2224; Diff = 1.5 mD].

Human V1a, human V2, human OTR and mouse V1a binding affinity measurement

The human and mouse receptors were cloned by RT-PCR from total human liver RNA (V1a), kidney RNA (V2), mammary gland RNA (OTR) or mouse liver RNA (mouse V1a). Cell membranes were prepared from HEK293 cells transiently transfected with expression vector coding for human V1a, human V2 or mouse V1a. For human OTR membrane preparation, a stable HEK clone expressing the receptor was selected. The transient or stable cells were grown in 20 liter fermenters.

For each receptor 50 g of cell pellet were resuspended in 30 mL ice cold Lysis buffer (50 mM HEPES, 1mM EDTA, 10 mM $MgCl_2$ adjusted to pH = 7.4 + complete cocktail of protease

inhibitor (Roche Diagnostics) and homogenized with Polytron for 1min The preparation was centrifuged 20 min at 500 g at 4 °C, the pellet discarded and the supernatant centrifuged 1 hour at 43'000 g at 4 °C (19'000 rpm). The pellet was resuspended in Lysis buffer + Sucrose 10%. The protein concentration was determined by the Bradford method and aliquots stored at -80 °C until use.

For vasopressin receptor binding studies 60mg Yttrium silicate SPA beads (Amersham) were mixed with an aliquot of membrane in binding buffer (50 mM Tris, 120 mM NaCl, 5 mM KCl, 2 mM $CaCl_2$, 10 mM $MgCl_2$) for 15 minutes with mixing. 50 μL of bead/membrane mixture was then added to each well of a 96 well plate, followed by 50 μL of 4 nM ^{3}H-Vasopressin (American Radiolabeled Chemicals). For total binding measurement 100 μL of binding buffer were added to the respective wells, for non-specific binding 100 μL of 8.4 mM cold vasopressin or cold oxytocin for hOTR and for compound testing 100 μL of a serial dilution of each compound in 2% DMSO. The plate was incubated 1 h at room temperature, centrifuged 1 min at 1000 g and counted on a Packard Top-Count.

Binding to human OTR was measured by filtration binding using 1nM ^{3}H-Oxytocin final concentration in Tris 50 mM, MgCl2 5 mM, 0.1% BSA (pH 7.4) buffer containing membranes. After compound addition as above and 1 hour incubation at room temperature, the binding was terminated by rapid filtration under vacuum through GF/C filters, presoaked for 5 min with assay buffer, and washed 5 times with ice-cold assay buffer before counting. Non-specific binding counts were subtracted from each well and data normalized to the maximum specific binding set at 100%.To calculate the IC50, the curve was fitted using a non-linear regression model (XLfit), and the Ki calculated using the Cheng-Prussoff equation. Saturation binding experiments

performed for each assay indicated that a single homogenous population of binding sites was being labelled. For receptor binding affinity (Ki) determination, compounds were tested at least 2 times in duplicate, important compounds were tested between 3 and 5 times in duplicate.

Stable cell culture and human V1a calcium flux assay using fluorescent imaging

CHO cells were stably transfected with expression plasmids encoding human V1a and grown in F-12 K, containing 10% fetal bovine serum, 1% penicillin-streptomycin, 1% L-glutamate, 200 ug/ml Geneticin at 37ºC in a 10% CO_2 incubator at 95% humidity.

Cells plated for 24h at 50,000 cells/well in clear bottom 96 well plates, were dye loaded for 60 minutes with 2 µM Fluo-4-AM in assay buffer. After cell washing, the plate was loaded on a Fluorometric Imaging Plate Reader (FLIPR), compound dilution series added to the cells and agonist activity measured. None of the compounds tested had agonistic activity. After 20 minutes incubation, a concentration of vasopressin (V1a agonist) giving 80% of the maximum signal was added to the plate and the calcium signal recorded for 5 minutes.

The calcium signal reduction due to the antagonist activity of the compounds was fitted to a single site competition equation with formula y = A + ((B-A)/(1+((x/C)D))), where y is the % normalized fluorescence, A is the minimum y, B is the maximum y, C is the IC50 (concentration inhibiting 50% of the agonist induced fluorescence), x is the log10 of the concentration of the competing compound and D the Hill Coefficient. IC50 values were transformed in apparent Kb values using the formula: Kb= IC50/ 1+(Agonist EC80/Agonist EC50). Agonist EC80 and EC50 were determined on the same day and the same cells in an independent experiment. For functional antagonism (Kb) determination, all compounds were

tested at least 2 times in duplicate, important compounds were tested between 3 and 5 times in duplicate.

Inhibition of AVP induced scratching in mice.

NMRI male mice (19-21 g) were used with n=8 per dose. Animals received an injection of either a potential V1a antagonist (different doses i.c.v. or i.p.- 5 or 30 min. prior to AVP treatment respectively), or vehicle. AVP was then administered (i.c.v.) under a short isoflurane anesthesia at a dose of 3ng / 5 μL two minutes prior to behavioral testing. Animals were then observed for 5 minutes, and the time spent on scratching was recorded. AVP was dissolved in artificial CSF (cerebrospinal fluid); V1a antagonists were administered i.p. in a 0.3% tween 80 in NaCl 0.9% solution or i.c.v. in artificial CSF.

Lipophilicity (log D) determination by high-throughput shake-flask

The applied methods called CAMDIS© (**CA**rrier **M**ediated **DI**stribution **S**ystem) for the determination of distribution coefficients are derived from the conventional 'shake flask' method. CAMDIS© is carried out in 96-well microtiterplates in combination with the novel DIFI©-tubes constructed by Roche, which provide a hydrophobic layer for the octanol phase. The experiment starts with the accurate coating of the hydrophobic layer (0,45 mm PVDF membranes), which is fixed on the bottom of each DIFI©-tube: Each membrane is impregnated with exactly 1.0 ml 1-octanol by a robotic system (Microfluidic Dispenser BioRAPTR, Bechman Coulter) . To expand the measurement range down to logD= -0.5, the procedure is carried at two different octanol/water ratios. One with a overplus of octanol for hydrophilic compounds (logD<1) and one with a low volume of octanol for the lipophilic compounds (logD>1).

Therefore, some DIFI©-tubes are filled with 15 µl 1-octanol. The coated membranes are then connected to a 96-well plate which has been prefilled with exactly 150 ml of the selected aqueous buffer solution (25 mM Phosphate, pH 7.4). The buffer solution contains already the compound of interest with a starting concentration of 100 mM. The resulting sandwich construct guarantees, that the membrane is completely dipped in the buffered sample solution. The plate is then sealed and shaken for 24 hours at room temperature (23°C). During this time the substance is distributed between the layer, the octanol and the buffer solution. After distribution equilibrium is reached the DIFI©-tubes are easly disassembled from the top of the 96-well plate, so that the remaining sample concentration in the aqueous phase can be analyzed by LC/MS. In order to know the exact sample concentration before incubation with 1-octanol, a part of the sample solution is connected to DIFI©-tubes without impregnation. The distribution coefficient is then calculated from the difference in concentration in the aqueous phase with and without impregnation and the ratio of the two phases. The preparation of the sample solutions is carried out by a TECAN robotic system (RSP 100, 8 channels).

Solubility determination (Lysa assay)

Samples are prepared in duplicate from 10 mM DMSO stock solutions. After evaporation (1h) of DMSO with a centrifugal vacuum evaporator (Genevac Technologies), the compounds are solved in 0.05 M phosphate buffer (pH 6.5), stirred for one hour and shaked for two hours. After one night, the solutions are filtered using a microtiter filter plate (Millipore MSDV N65) and the filtrate and its 1/10 dilution are then analyzed by direct UV measurement or by HPLC-UV.

In addition a four point calibration curve is prepared from the 10 mM stock solutions and used for the solubility determination of the compounds. Starting from 10 mM stock solution, the measurement range for MW 500 is 0- 666 µg/ml.

ASSOCIATE CONTENT

Supporting Information

CEREP selectivity screening data for **8**. NMR spectra and LC-HRMS report for **8**. Synthetic scheme of compounds **33** and **34**. A pdb file with the coordinates of the ligands and full V1a receptor. This material is free of charge via the Internet at http://pubs.acs.org.

AUTHORS INFORMATION

Corresponding Authors

*Hasane Ratni. E-mail: hasane.ratni@roche.com; Phone: (+41) 61-688-2748. *Mark Rogers-Evans. Email: mark.rogers-evans@roche.com; Phone: (+41) 61-688-2245. Chemogenomic and modeling contact author. *Caterina Bissantz. E-mail: caterina.bissantz@roche.com; Phone: (+41) 61-687-8657.

Note

The authors declare the following competing financial interest(s): The authors are or have been employees of F. Hoffmann-La Roche AG.

ACKNOWLEDGMENTS

We thank Angelique Patiny-Adam, Philippe Jablonski, Didier Rombach, Fabienne Vannay, Radouane Souissi, Rafael Flückiger, Gabriela Schnider and Cosimo Dolente for the synthesis of the compounds described, Muriel Schmitt, Alain Rudler, Gabrielle Py and Andy Stucki for the *in vitro* affinity and potency assessments, Hoa Truong and Martin Graf for the HTS, Josef Schneider for the NMR spectroscopy, Christian Bartelmus for the mass spectroscopy and Tanja Schulz-Gasch for preparing the table of contents graphic. The research described in the manuscript was funded by F. Hoffmann-La Roche AG.

ABBREVIATIONS USED

AVP; Arginine vasopressin; DMAP, *N*,*N*-dimethylpyridin-4-amine; DMF, *N*,*N*-dimethylformamide; EDC, 1-(3-Dimethylaminopropyl)-3-ethylcarbodiimide hydrochloride; GPCR, G-protein coupled receptor; HATU, O-(7-Azabenzotriazol-1-yl)-N,N,N',N'-tetramethyluronium hexafluorophosphate; HOBt, 1-Hydroxybenzotriazole hydrate; HRMS, High resolution mass spectrometry; HTS, high throughput screening; i.c.v., intra-cerebro-ventricular; i.p., intraperitoneal; NMR, Nuclear magnetic resonance; OT, Oxytocin; PC, Prinipal Components; P-gp, P-glycoprotein; RT, Room temperature; SPA, Scintillation Proximity Assay; TFA, Trifluoroacetic acid; TFAA, Trifluoroacetic anhydride; THF, Tetrahydrofuran; V1a, Vasopressin 1a; V2, Vasopressin 2.

REFERENCES

1. Insel, T. R. The challenge of translation in social neuroscience: A review of oxytocin, vasopressin, and affiliative behavior. *Neuron* **2010,** *65*, 768-779.

2. Ebner, K.; Wotjak, C. T.; Landgraf, R.; Engelmann, M. Forced swimming triggers vasopressin release within the amygdala to modulate stress-coping strategies in rats. *Eur. J. Neurosci.* **2002,** *15*, 384-388.

3. Liebsch, G.; Wotjak, C. T.; Landgraf, R.; Engelmann, M. Septal vasopressin modulates anxiety-related behaviour in rats. *Neurosci. Lett.* **1996,** *217*, 101-104.

4. Zink, C. F.; Stein, J. L.; Kempf, L.; Hakimi, S.; Meyer-Lindenberg, A. Vasopressin modulates medial prefrontal cortex–amygdala circuitry during emotion processing in humans. *J. Neurosci.* **2010,** *30*, 7017-7022.

5. Thompson, R.; Gupta, S.; Miller, K.; Mills, S.; Orr, S. The effects of vasopressin on human facial responses related to social communication. *Psychoneuroendocrinology* **2004,** *29*, 35-48.

6. Loup, F.; Tribollet, E.; Dubois-Dauphin, M.; Dreifuss, J. J. Localization of high-affinity binding sites for oxytocin and vasopressin in the human brain. An autoradiographic study. *Brain Res.* **1991,** *555*, 220-232.

7. Young, L. J.; Toloczko, D.; Insel, T. R. Localization of vasopressin (V1a) receptor binding and mRNA in the rhesus monkey brain. *J. Neuroendocrinol.* **1999,** *11*, 291-297.

8. (a) Ostrowski, N. L.; Lolait, S. J.; Bradley, D. J.; O'Carroll, A. M.; Brownstein, M. J.; Young, W. S. 3rd. Distribution of V1a and V2 vasopressin receptor messenger ribonucleic acids in rat liver, kidney, pituitary and brain. *Endocrinology* **1992,** *131*, 533-535; (b) Ostrowski, N. L.; Lolait, S. J.; Young, W. S. 3rd. Cellular localization of vasopressin V1a receptor messenger ribonucleic acid in adult male rat brain, pineal, and brain vasculature. *Endocrinology* **1994,** *135*, 1511-1528.

9. Lolait, S. J.; O'Carroll, A. M.; Mahan, L. C.; Felder, C. C.; Button, D. C.; Young, W. S., 3rd; Mezey, E.; Brownstein, M. J. Extrapituitary expression of the rat V1b vasopressin receptor gene. *Proc. Natl. Acad. Sci. U. S. A.* **1995,** *92*, 6783-6787.

10. Kimura, T.; Tanizawa, O.; Mori, K.; Brownstein, M. J.; Okayama, H. Structure and expression of a human oxytocin receptor. *Nature* **1992,** *356*, 526-529.

11. Ryckmans, T. Modulation of the vasopressin system for the treatment of CNS diseases. *Curr. Opin. Drug Discovery Dev.* **2010,** *13*, 538-547.

12. (a) Serradeil-Le Gal, C.; Herbert, J. M.; Delisee, C.; Schaeffer, P.; Raufaste, D.; Garcia, C.; Dol, F.; Marty, E.; Maffrand, J. P.; Le Fur, G. Effect of SR-49059, a vasopressin V1a antagonist, on human vascular smooth muscle cells. *Am. J. Physiol.* **1995,** *268*, H404-H410; (b) Serradeil-Le Gal, C.; Wagnon, J.; Garcia, C.; Lacour, C.; Guiraudou, P.; Christophe, B.; Villanova, G.; Nisato, D.; Maffrand, J. P.; Le Fur, G.: Guillon, G.; Cantau, B.; Barberis, C.; Trueba, M.; Ala, Y.; Jard, S. Biochemical and pharmacological properties of SR 49059, a new, potent, nonpeptide antagonist of rat and human vasopressin V1a receptors. *J. Clin. Invest.* **1993,** *92*, 224-231.

13. Decaux, G.; Soupart, A.; Vassart, G. Non-peptide arginine-vasopressin antagonists: the vaptans. *Lancet* **2008,** *371*, 1624-1632.

14. Johnson, P. S.; Ryckmans, T.; Bryans, J.; Beal, D. M.; Dack, K. N.; Feeder, N.; Harrison, A.; Lewis, M.; Mason, H. J.; Mills, J.; Newman, J.; Pasquinet, C.; Rawson, D. J.; Roberts, L. R.; Russell, R.; Spark, D.; Stobie, A.; Underwood, T. J.; Ward, R.; Wheeler, S. Discovery of PF-184563, a potent and selective V1a antagonist for the treatment of dysmenorrhoea. The influence of compound flexibility on microsomal stability. *Bioorg. Med. Chem. Lett.* **2011,** *21*, 5684-5687.

15. (a) Fabio, K.; Guillon, C.; Lacey, C. J.; Lu, S.-f.; Heindel, N. D.; Ferris, C. F.; Placzek, M.; Jones, G.; Brownstein, M. J.; Simon, N. G. Synthesis and evaluation of potent and selective human V1a receptor antagonists as potential ligands for PET or SPECT imaging. *Bioorg. Med. Chem.* **2012,** *20*, 1337-1345; (b) Fabio, K. M.; Guillon, C. D.; Lu, S.-f.; Heindel, N. D.; Brownstein, M. J.; Lacey, C. J.; Garippa, C.; Simon, N. G. Pharmacokinetics and metabolism of SRX246: A potent and selective vasopressin 1a antagonist. *J. Pharm. Sci.* **2013,** *102*, 2033-2043; (c) Lee, R. J.; Coccaro, E. F.; Cremers, H.; McCarron, R.; Lu, S.-F.; Simon, N. G.; Brownstein, M. J. A novel V1a receptor antagonist blocks vasopressin-induced changes in the CNS response to emotional stimuli: an fMRI study. *Front. Syst. Neurosci.* **2013,** *7*, 100.

16. (a) Ferris, C. F.; Lu, S.-f.; Messenger, T.; Guillon, C. D.; Heindel, N.; Miller, M.; Koppel, G.; Bruns, F. R.; Simon, N. G. Orally active vasopressin V1a receptor antagonist, SRX251, selectively blocks aggressive behavior. *Pharmacol. Biochem. Behav.* **2006,** *83*, 169-174; (b) Ferris, C. F.; Stolberg, T.; Kulkarni, P.; Murugavel, M.; Blanchard, R.; Blanchard, D. C.; Febo, M.; Brevard, M.; Simon, N. G. Imaging the neural circuitry and chemical control of aggressive motivation. *BMC Neurosci.* **2008,** *9*, DOI10.1186/1471-2202-9-111

17. https://clinicaltrials.gov/ct2/show/NCT02055638

18. Bleickardt, C. J.; Mullins, D. E.; MacSweeney, C. P.; Werner, B. J.; Pond, A. J.; Guzzi, M. F.; Martin, F. D. C.; Varty, G. B.; Hodgson, R. A. Characterization of the V1a antagonist, JNJ-17308616, in rodent models of anxiety-like behavior. *Psychopharmacology (Berlin, Ger.)* **2009,** *202*, 711-718.

19. (a) Arbuckle, W.; Baker, J.; Barn, D.; Bingham, M.; Brown, A.; Buchanan, K.; Craighead, M.; Goodwin, R.; Goutcher, S.; Kiczun, M.; Lyons, A.; Milne, R.; Montgomery, B.; Napier, S.; Presland, J.; Sloan, H.; Turnbull, Z.; Wishart, G. Optimisation of pharmacokinetic

properties to afford an orally bioavailable and selective V1A receptor antagonist. *Bioorg. Med. Chem. Lett.* **2011,** *21*, 4622-4628; (b) Napier, S.; Wishart, G.; Arbuckle, W.; Baker, J.; Barn, D.; Bingham, M.; Brown, A.; Byford, A.; Claxton, C.; Craighead, M.; Buchanan, K.; Fielding, L.; Gibson, L.; Goodwin, R.; Goutcher, S.; Irving, N.; MacSweeney, C.; Milne, R.; Mort, C.; Presland, J.; Sloan, H.; Thomson, F.; Turnbull, Z.; Young, T. The discovery of novel 8-azabicyclo[3.2.1]octan-3-yl)-3-(4-chlorophenyl) propanamides as vasopressin V1A receptor antagonists. *Bioorg. Med. Chem. Lett.* **2011,** *21*, 3163-3167.

20. (a) Bissantz, C.; Grundschober, C.; Masciadri, R.; Ratni, H.; Rogers-Evans, M.; Schnider, P. Preparation of indolylcarbonylazaspiropiperidines as vasopressin VIa receptor antagonists. US20080161332A1, 2008; (b) Bissantz, C.; Grundschober, C.; Ratni, H.; Rogers-Evans, M.; Schnider, P. Indole-3-carbonyl-spiro-piperidine derivatives as V1a receptor antagonists and their preparation, pharmaceutical compositions and use in the treatment of diseases. WO2007006688A1, 2007; (c) Bissantz, C.; Grundschober, C.; Ratni, H.; Rogers-Evans, M.; Schnider, P. Preparation of indol-3-ylcarbonylspiropiperidines as vasopressin V1a receptor antagonists. US20070155761A1, 2007; (d) Bissantz, C.; Grundschober, C.; Ratni, H.; Rogers-Evans, M.; Schnider, P. Preparation of (indole-3-carbonylpiperidinyl)benzimidazoles as vasopressin receptor V1a antagonists, their pharmaceutical compositions and use in treatment of diseases. WO2007009906A1, 2007; (e) Bissantz, C.; Grundschober, C.; Ratni, H.; Rogers-Evans, M.; Schnider, P. Preparation of indol-3-yl-carbonyl piperidine and piperazine derivatives as V1a vasopressin receptor antagonists. US20070027163A1, 2007.

21. (a) Cipiciani, A.; Clementi, S.; Linda, P.; Savelli, G.; Sebastiani, G. V. Unusual site of electrophilic attack on indole and carbazole. *Tetrahedron* **1976,** *32*, 2595-2597; (b) Swain, C. J.; Baker, R.; Kneen, C.; Moseley, J.; Saunders, J.; Seward, E. M.; Stevenson, G.; Beer, M.;

Stanton, J.; Watling, K. Novel 5-HT3 antagonists. Indole oxadiazoles. *J. Med. Chem.* **1991,** *34*, 140-151.

22. Braghiroli, D.; Avallone, R.; Di Bella, M. Asymmetric synthesis of (R)- and (S)-2-pyrrolidinemethanesulfonic acid. *Tetrahedron: Asymmetry* **1997,** *8*, 2209-2213.

23. Apweiler, R.; Bairoch, A.; Wu, C. H.; Barker, W. C.; Boeckmann, B.; Ferro, S.; Gasteiger, E.; Huang, H.; Lopez, R.; Magrane, M.; Martin, M. J.; Natale, D. A.; O'Donovan, C.; Redaschi, N.; Yeh, L.-S. L. UniProt: the universal protein knowledgebase. *Nucleic Acids Res.* **2004,** *32*, D115-D119.

24. Bissantz, C.; Logean, A.; Rognan, D. High-throughput modeling of human g-protein coupled receptors: Amino acid sequence alignment, three-dimensional model building, and receptor library screening. *J. Chem. Inf. Comput. Sci.* **2004,** *44*, 1162-1176.

25. Kratochwil, N. A.; Malherbe, P.; Lindemann, L.; Ebeling, M.; Hoener, M. C.; Muehlemann, A.; Porter, R. H. P.; Stahl, M.; Gerber, P. R. An automated system for the analysis of G protein-coupled receptor transmembrane binding pockets: Alignment, receptor-based pharmacophores, and their application. *J. Chem. Inf. Model.* **2005,** *45*, 1324-1336.

26. Sandberg, M.; Eriksson, L.; Jonsson, J.; Sjoestroem, M.; Wold, S. New chemical descriptors relevant for the design of biologically active peptides. A multivariate characterization of 87 amino acids. *J. Med. Chem.* **1998,** *41*, 2481-2491.

27. Hopkins, A. L.; Keserue, G. M.; Leeson, P. D.; Rees, D. C.; Reynolds, C. H. The role of ligand efficiency metrics in drug discovery. *Nat. Rev. Drug Discovery* **2014,** *13*, 105-121.

28. Malherbe, P.; Bissantz, C.; Marcuz, A.; Kratzeisen, C.; Zenner, M.-T.; Wettstein, J. G.; Ratni, H.; Riemer, C.; Spooren, W. Me-talnetant and osanetant interact within overlapping but

not identical binding pockets in the human tachykinin neurokinin 3 receptor transmembrane domains. *Mol. Pharmacol.* **2008,** *73*, 1736-1750.

29. (a) Meisenberg, G. Vasopressin-induced grooming and scratching behavior in mice. *Ann. N. Y. Acad. Sci.* **1988,** *525*, 257-269; (b) Lumley, L. A.; Robison, C. L.; Chen, W. K.; Mark, B.; Meyerhoff, J. L. Vasopressin into the preoptic area increases grooming behavior in mice. *Physiol. Behav.* **2001,** *73*, 451-455.

30. Bielsky, I. F.; Hu, S.-B.; Szegda, K. L.; Westphal, H.; Young, L. J. Profound impairment in social recognition and reduction in anxiety-like behavior in vasopressin V1a receptor knockout mice. *Neuropsychopharmacology* **2004,** *29*, 483-493.

31. Data for CEREP screen for RO5028442 available in the supporting information

32. http://clinicaltrials.gov/ct2/show/NCT01474278

33. Sommer, M. B.; Nielsen, O. Method for manufacture of dihydroisobenzofuran derivatives, useful as drug intermediates, via Grignard reaction and ring closure of the obtained diols. WO2004026855A1, 2004.

34. Brown, A. D.; Calabrese, A. A.; Ellis, D. Preparation of 1,2,4-triazole derivatives as oxytocin antagonists. WO2006092731A1, 2006.

35. Kubota, H.; Kafefuda, A.; Nagaoka, H.; Yamamoto, O.; Ikeda, K.; Takeuchi, M.; Shibanuma, T.; Isomura, Y. Spiro-substituted piperidines as neurokinin receptor antagonists. II. Syntheses and NK2 receptor-antagonistic activities of N-[2-aryl-4-(spiro-substituted piperidin-1'-yl)butyl]carboxamides. *Chem. Pharm. Bull.* **1998,** *46*, 242-254.

Table of Contents Graphic